RECLAMATION

Managing Water in the West

Trinity River 40 Mile Hydraulic Model: Development and Analysis

Technical Service Center
Sedimentation and River Hydraulics Group
Technical Report No. SRH-2016-27

U.S. Department of the Interior
Bureau of Reclamation
Research and Development Office

8/25/2015

Mission Statements

The U.S. Department of the Interior protects America's natural resources and heritage, honors our cultures and tribal communities, and supplies the energy to power our future.

The mission of the Bureau of Reclamation is to manage, develop, and protect water and related resources in an environmentally and economically sound manner in the interest of the American public.

REPORT DOCUMENTATION PAGE		*Form Approved* *OMB No. 0704-0188*
T1. REPORT DATE 8/2016	**T2. REPORT TYPE** Research	**T3. DATES COVERED** **8/1/2014 – 9/30/2016**
T4. TITLE AND SUBTITLE **Trinity River 40 Mile Hydraulic Model: Development and Analysis** **Technical Report No. SRH-2016-27**		**5a. CONTRACT NUMBER** **5b. GRANT NUMBER** **5c. PROGRAM ELEMENT NUMBER**
6. AUTHOR(S) **D. Nathan Bradley**		**5d. PROJECT NUMBER** **5e. TASK NUMBER** **5f. WORK UNIT NUMBER** 86-68240
7. PERFORMING ORGANIZATION NAME(S) AND ADDRESS(ES) **Sedimentation and River Hydraulics Group** **Technical Service Center, Bureau of Reclamation, Denver, CO 80225**		**8. PERFORMING ORGANIZATION REPORT NUMBER**
9. SPONSORING / MONITORING AGENCY NAME(S) AND ADDRESS(ES) Trinity River Restoration Program PO Box 1300 1313 South Main Street Weaverville, CA 96093		**10. SPONSOR/MONITOR'S ACRONYM(S)** **TRRP: Trinity River Restoration Program** **11. SPONSOR/MONITOR'S REPORT NUMBER(S)**
12. DISTRIBUTION / AVAILABILITY STATEMENT **Final report can be downloaded from the TRRP's website: http://www.trrp.net/odp/**		
13. SUPPLEMENTARY NOTES		

14. ABSTRACT ***(Maximum 200 words)***

At the request of the Trinity River Restoration Program (TRRP), the Bureau of Reclamation's Sedimentation and River Hydraulics group developed a two-dimensional hydrodynamic model to predict the spatial patterns of water depth, velocity, and shear stress and to estimate the location, quantity, and quality of salmonid habitat in the Trinity River between Lewiston Dam and the junction with the North Fork. Model development began in the fall of 2013 and the latest version of the model was completed in the summer of 2015. The model has been used to select sites on the river for habitat restoration work, to evaluate proposed restoration designs, and as the hydraulic input to a fish production model. The hydraulic model is based on the surveyed topography and bathymetry of the Trinity River (performed in 2011 and 2012), estimates of channel and floodplain roughness, discharge from Lewiston dam and six tributaries, and the outlet water surface elevation for a given discharge. This report describes the development and analysis of the hydraulic model and the associated habitat module. All model runs described below are steady-state models that simulate a constant discharge over an immobile bed.

15. SUBJECT TERMS Uncertainty Analysis, Sediment Transport Modeling, Bayesian					
16. SECURITY CLASSIFICATION OF: U			**17. LIMITATION OF ABSTRACT**	**18. NUMBER OF PAGES**	**19a. NAME OF RESPONSIBLE PERSON D. Nathan Bradley**
a. REPORT U	**b. ABSTRACT** U	**c. THIS PAGE** U	**U**	57	**19b. TELEPHONE NUMBER** **303-445-2565**

S Standard Form 298 (Rev. 8/98)
P Prescribed by ANSI Std. 239-18

PEER REVIEW DOCUMENTATION

Report Title: Trinity River 40 Mile Hydraulic Model: Development and Analysis

Client: Trinity River Restoration Program

Technical Report No. SRH-2016-27

Prepared by:

D. Nathan Bradley Date: 8/31/16

D. Nathan Bradley, Ph.D.
Physical Scientist, Sedimentation and River Hydraulics Group (86-68240)

Review Certification

Peer Reviewer: I have reviewed the assigned items/sections(s) noted for the above document and believe them to be in accordance with the project requirements, standards of the profession, and Reclamation policy.

Date: 8-31-16

Blair Greimann, Ph.D., P.E.
Hydraulic Engineer, Sedimentation and River Hydraulics Group (86-68240)

Table of Contents

Table of Figures

Table of Tables

Acronyms and Abbreviations

2D	Two Dimensional
CDF	Cumulative Distribution Function
cfs	Cubic Feet per Second
D_{84}	84^{th} percentile of grain size
GRTS	Generalized Random Tessellation Stratified
HBLM	Hydrodynamic Based Logic Modelling Tool
Reclamation	Bureau of Reclamation
TRRP	Trinity River Restoration Program
SRH-2D	Sedimentation and River Hydraulics – Two-Dimensional
WSE	Water Surface Elevation
WUA	Weighted Useable Area

Citation:

Bradley, D. Nathan (2015). Trinity River 40 Mile Hydraulic Model: Development and Analysis, Technical Report No. SRH-2016-27, Prepared for Trinity River Restoration Program, August 2016.

Key Words: Trinity River, Hydraulic Modeling, Salmonid Habitat

Introduction

At the request of the Trinity River Restoration Program (TRRP), the Bureau of Reclamation's Sedimentation and River Hydraulics group developed a two-dimensional hydrodynamic model to predict the spatial patterns of water depth, velocity, and shear stress and to estimate the location, quantity, and quality of salmonid habitat in the Trinity River between Lewiston Dam and the junction with the North Fork. Model development began in the fall of 2013 and the latest version of the model was completed in the summer of 2015. The model has been used to select sites on the river for habitat restoration work, to evaluate proposed restoration designs, and as the hydraulic input to a fish production model.

The hydraulic model is based on the surveyed topography and bathymetry of the Trinity River (performed in 2011 and 2012), estimates of channel and floodplain roughness, discharge from Lewiston dam and six tributaries, and the outlet water surface elevation for a given discharge. This report describes the development and analysis of the hydraulic model and the associated habitat module. All model runs described below are steady-state models that simulate a constant discharge over an immobile bed.

Model Description

The Bureau of Reclamation's Sedimentation and River Hydraulics model (SRH-2D) is a two dimensional, depth averaged hydraulic model [*Lai*, 2008]. The model solves the depth-integrated, dynamic wave approximation of the Navier-Stokes fluid flow equations with a finite-volume numerical method. More information about SRH-2D can be found at http://www.usbr.gov/tsc/techreferences/computer%20software/models/srh2d/index.html.

Model Domain and Mesh Development

The first step in the development of a hydraulic model is the creation of a model mesh. The model mesh defines the model domain and discretizes the physical space represented by the model so that the differential equations describing the continuous physical process of fluid flow can be solved numerically between mesh elements. The mesh represents the underlying terrain by assigning elevations to the mesh nodes. Elevations were interpolated from the terrain model developed from the topographic and bathymetric surveys in 2011 and 2012. A few mesh nodes fall outside the boundaries of the terrain model. Elevations for these nodes are extrapolated from the elevations of neighboring nodes.

The model mesh also defines the spatial resolution of the model. The hydraulic variables computed by the model (water depth and velocity, for example) are spatially averaged over the area represented by each of the mesh elements. Smaller mesh elements average over a smaller area and are therefore better able to represent the slow, shallow water along the channel margins. Smaller mesh elements also represent variations in bed roughness and elevation in more detail. The downside to using smaller mesh elements is that more elements are required to cover a given area and consequently, the model requires more computation time. Developing a high resolution model mesh also takes more time and effort to develop. In other words, there is a trade-off between the model resolution and the time required for mesh development and computation of a solution.

The first version of the Trinity River hydraulic model was developed in late 2013 and 2014 and contained about 900,000 mesh elements. The modal size of channel mesh elements was about 50 ft^2 (5 ft. wide by

10 ft. in the streamwise direction). This version of the model was used as the basis of the Hydrodynamic Based Logic Modelling Tool (HBLM) [*Bandrowski et al.*]. Analysis of this version of the model showed that the model water velocity estimates along the channel margins were higher than those observed in the river and therefore the model underestimated the amount of juvenile salmonid habitat.

To improve the model's habitat estimates, we developed second version of the model, referred to variously as the latest version, the 2nd version, or the fish production hydraulic model. This version of the model uses a mesh with a bi-modal distribution of channel mesh element sizes. The mesh includes bands of smaller quadrilateral elements between the 300 cubic feet per second (cfs) water's edge and the 4500 cfs water's edge. These smaller elements, typically about 2 ft. wide and 10 ft. long, are intended to better represent the slow and shallow water favored by juvenile salmonids. Mesh elements in the middle of the channel are typically about 10 ft. by 10 ft. This meshing approach was tested first on the Lower Valley restoration sites (Chapman Ranch to Sheridan Creek) and the results were promising enough that the decision was made to extend the new mesh to the entire 40 miles below Lewiston. This version of the mesh contains more than two million elements. Figure 1 shows the model mesh near Roundhouse.

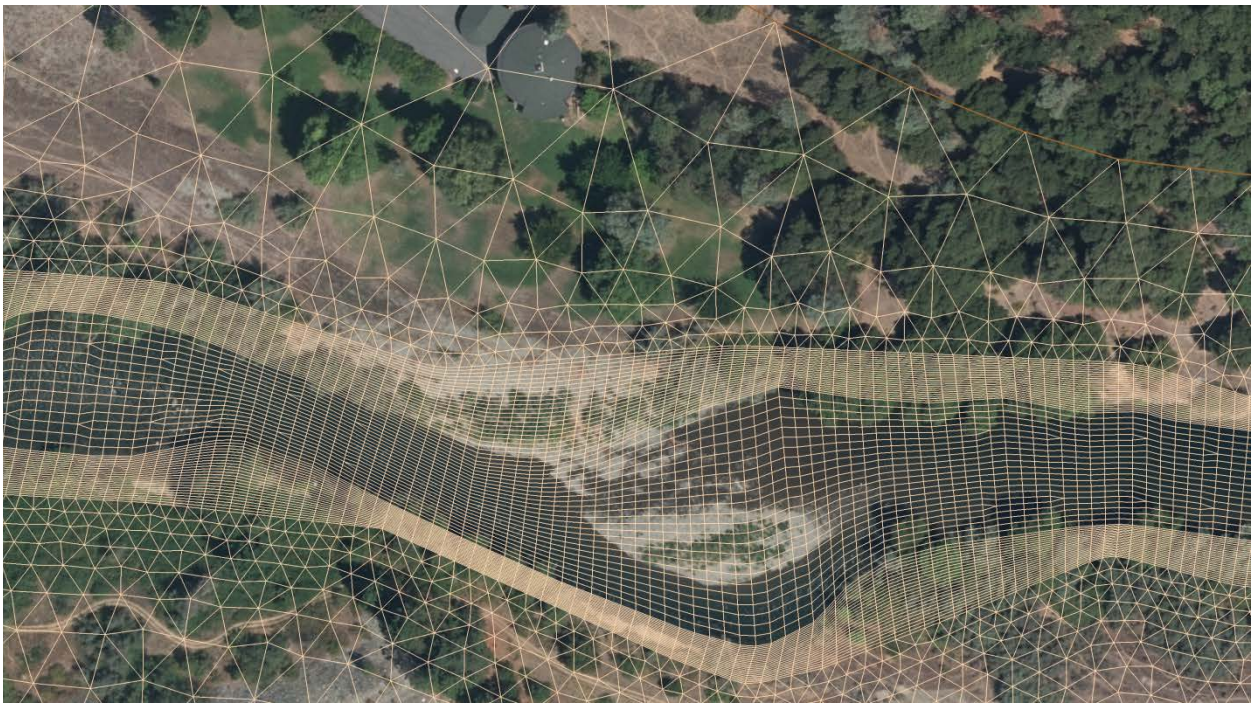

Figure 1. The new model mesh showing the bands of smaller mesh elements along the channel margins at the upstream end of Chapman Ranch, near Roundhouse.

Boundary Conditions

Boundary conditions define how water enters and exits the model domain. The inlet boundary condition is the amount of water in cubic feet per second flowing into the model domain that is to be simulated, and is therefore prescribed by the user. We modeled 18 dam releases ranging from 300 cfs to 11,000 cfs, 7 winter baseflow (300 cfs at Lewiston) tributary accretion flows based on tributary gage records, and 1 summer baseflow with tributary accretion. Tributary accretion is described in detail in Appendix A.

The outlet boundary condition is the water surface elevation at the outlet boundary for the discharge being simulated. A linear rating curve of water surface elevation at the junction with the North Fork was developed for discharges up to 11,000 cfs based on observations. The rating curve is shown in Figure 2.

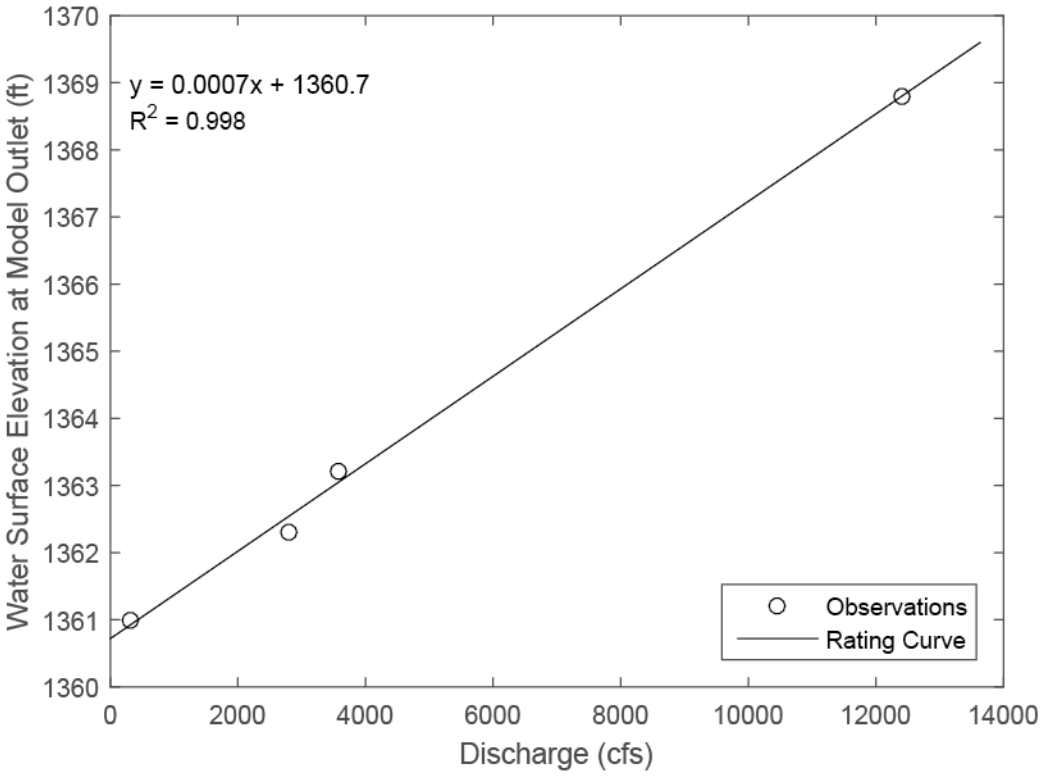

Figure 2. Rating curve of water surface elevation at the junction with the North Fork.

Flow Resistance and Model Calibration

SRH-2D represents the friction between the flowing water and the bed and banks of the channel with Manning's roughness coefficient (Manning's n). A value of Manning's n is assigned to each mesh element. The channel roughness is SRH-2D's primary tuning parameter to adjust the model water surface elevations and velocities to observed values. While it is possible to adjust the roughness on an element-by-element basis, it is more practical to assign values over broad areas of similar morphology, such as gravel bars, main channel, or side channels.

We calibrated the first version of the model by adjusting Manning's n to match water surface elevation observations made during the bathymetric survey. The calibration procedure was to adjust the channel roughness to eliminate broad areas of systematic disagreement with the observations. The observations took place at discharges ranging from 500 cfs to 4500 cfs, so each part of the model is calibrated only to the particular flow at the time that section of river was surveyed. Calibrating the model to water surface observations of the entire 40 miles surveyed at a variety of flows would have been a better approach, but those data were not available. Table 1 lists the flows and survey dates used in the model calibration. Figure 3 shows the probability distribution of water surface elevation residuals (model water surface elevation minus observed elevation). The mean of elevation residuals is -0.017 ft. and the standard deviation is 0.29 ft. The model water surface is within +/- 0.5 ft. of 91% of the observations and is nearly symmetrical around zero. This error in the model water surface is similar to the reported error of the bathymetric and topographic elevations [*Graham Matthews and Associates*, 2012; *Woolpert*, 2013]. Figure 4 shows the same data plotted against distance from Lewiston Dam. Table 2 lists the values of Manning's n used to calibrate the first version of the model.

Table 1. The flows used for calibrating the model.

Release from Lewiston (cfs)	**Survey Date**
500	Sept 27-29, 2011
1200	July 11-12, 2012
1300	July 5-10, 2011
1600	July 2-5, 2011
2000	June 12-24, 2011 June 19-28, 2012
2500	June 8-10, 2011 April 29-May 4, 2012 June 6-16, 2012
4500	May 17-18, 2012

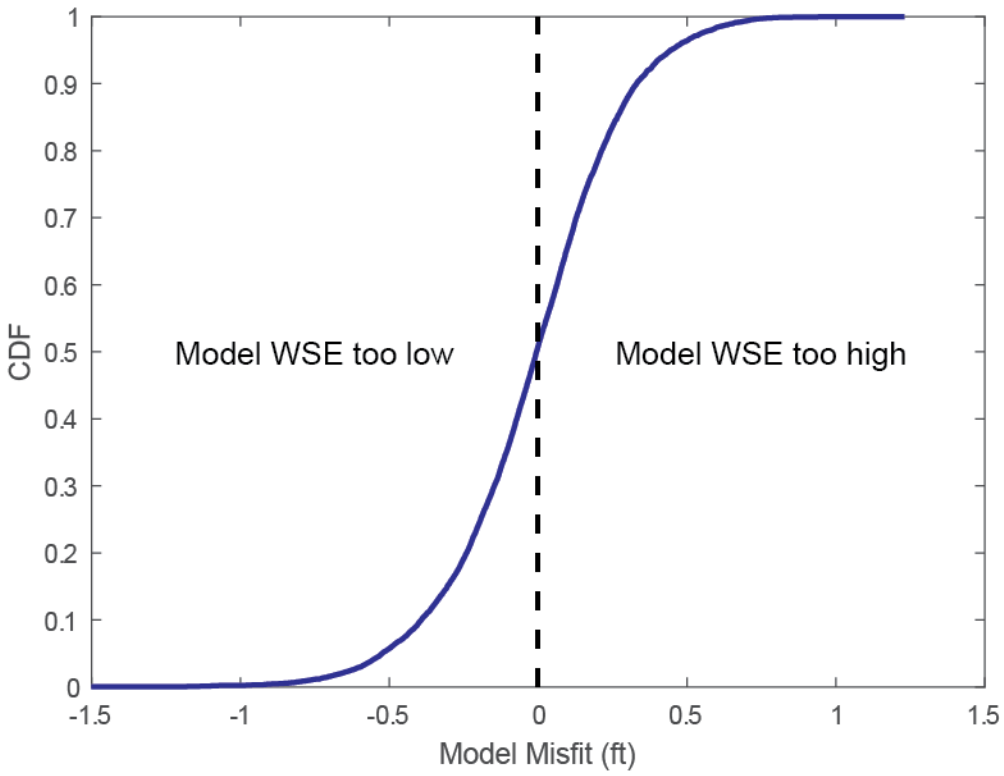

Figure 3. The cumulative probability distribution of water surface elevation residuals used to evaluate the calibration of the first version of the model. The mean of elevation residuals is -0.017 ft. and the standard deviation is 0.29 ft. The model water surface is within +/- 0.5 ft. of 91% of the observations. It is within +/- 1 ft. of 99.7% of the observations.

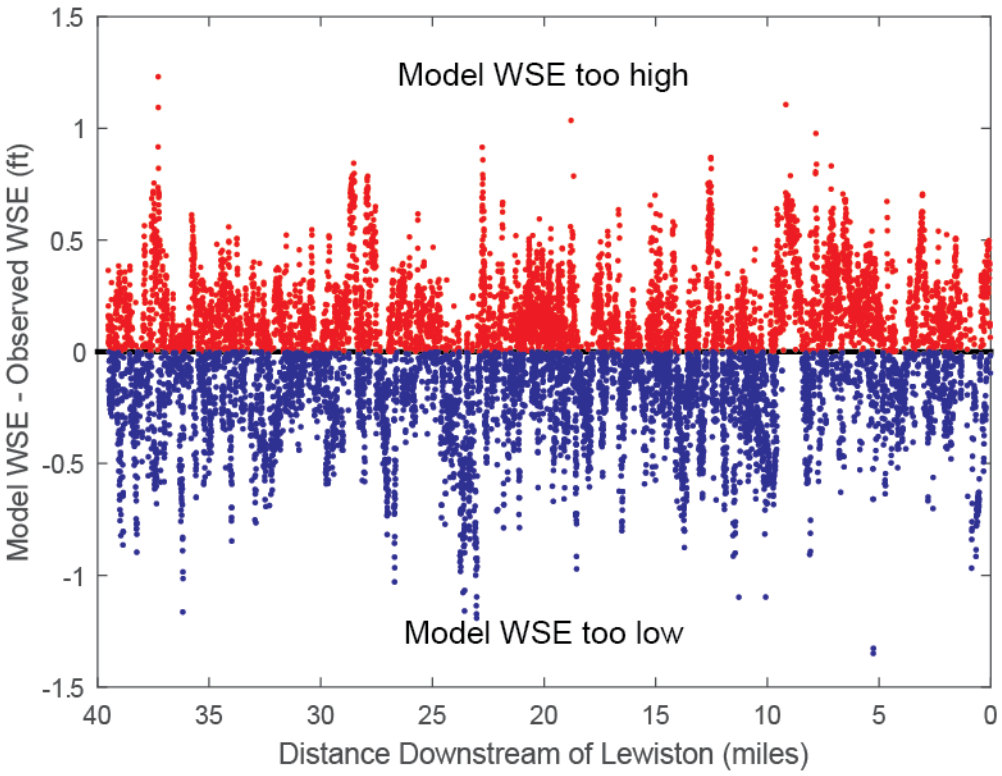

Figure 4. The water surface elevation residuals from the first version of the model plotted vs. distance from Lewiston dam. Plots like this one were used during the calibration process to eliminate broad areas of systematic disagreement with the observations by adjusting the channel roughness.

Table 2. Values of Manning's n used to calibrate the first version of the model.

Geomorphic Element	Manning's n
Smoother Main Channel	0.025
Smooth Main Channel	0.0275
Main Channel	0.03
Main Channel Riffle	0.035
Rough Main Channel	0.035
Rougher Main Channel	0.04
Gravel Bar	0.03
Vegetated Gravel Bar	0.04
Side Channel	0.035
Slackwater	0.025
Tributary	0.03
Floodplain	0.07

In the second version of the model, we chose to develop the channel roughness from the physical characteristics of the channel and established relationships between those characteristics and flow resistance. Specifically, we used observations of sediment grain size, in-channel vegetation and wood, and riparian vegetation to develop detailed roughness maps.

The primary dataset used to develop the channel roughness is the map of the 84th percentile of sediment grain size (D_{84}) within the 2000 cfs flow boundary developed by the Trinity River Habitat Assessment Team in 2014 [*Alvarez et al.*, 2015]. The map of D_{84} was converted to a map of Manning's n according to the following equation from *López and Barragán* [2008] and *García* [2008]

$$n = \frac{C_m(2.8D_{84})^{\frac{1}{6}}}{\left(8.1\sqrt{g}\right)}$$

where C_m is the unit conversion factor in the Manning equation, equal to 1 for SI units, g is the acceleration of gravity, and D_{84} is in meters. The continuous map of Manning's n was interpolated to the locations of the model mesh element centroids and discretized to roughly 50 unique values by binning into 0.001 wide bins. This step is necessary because SRH-2D limits the number of unique values of Manning's n allowed in a mesh.

The second dataset used in the development of the roughness map is the in-water cover map developed by the habitat team (delivered by Aaron Martin on April 23, 2015). This map outlines material within the 450 cfs flow boundaries, typically wood, that provides escape cover for juvenile fish and increases flow resistance. Mesh elements within the cover polygons were assigned a value of n=0.04. This value was chosen because assigning higher roughness values to in-water cover elements caused the water surface elevation to increase by an unrealistic amount.

The final dataset used in estimating flow resistance is the map of the 2014 riparian vegetation outside of the 450 cfs flow boundary [*HVT and McBain Associates*, 2015]. Aaron Martin and others developed roughness polygon values based on the vegetation type and the floodplain was assigned Manning's n values of 0.025, 0.045, 0.06, or 0.08 based on these polygons.

Habitat Calculations

SRH-2D includes a habitat module, a post-processing option that analyzes the hydraulic results in the context of juvenile salmonid habitat. Among other things, the habitat module classifies each model cell into one of three habitat suitability classes based on thresholds of water depth, water velocity, and distance to cover (e.g., vegetation or in-water features such as large wood). The distance to cover computation requires a shapefile designating cover polygons. The shapefile used in the calculations was derived from the riparian vegetation map used to assign floodplain roughness clipped to the 450 cfs bank lines and the in-water cover map used to assign roughness to in-channel elements such as large wood.

In addition to the output of the habitat module, we also evaluated habitat suitability based on continuous habitat suitability curves developed using the methodology described by *Som et al.* [2015]. An example of the suitability curves is shown in Figure 5. Each element was assigned a score based on the average of the depth, velocity, and distance to cover score. The score was then weighted by the element area and

summed over a particular site on the river to yield a Weighted Useable Area (WUA) that represents the amount of habitat at that site.

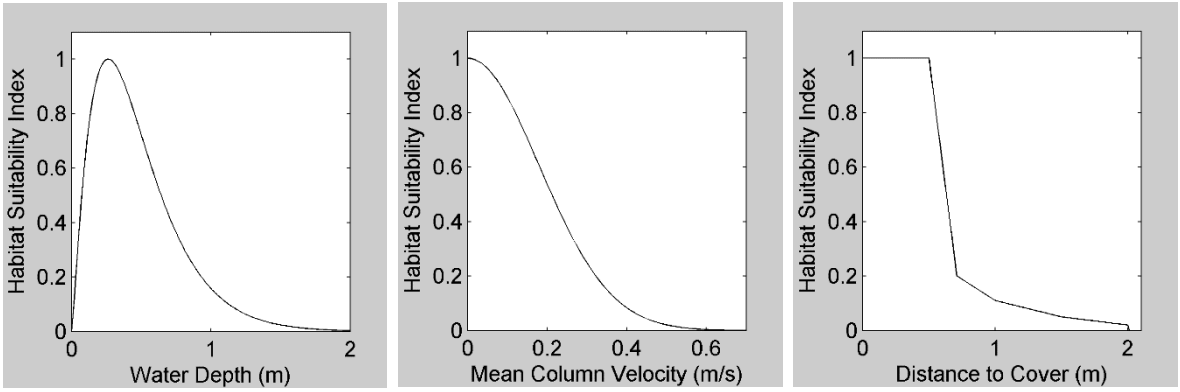

Figure 5. Habitat suitability curves use to evaluate juvenile salmonid habitat

Quantitative Evaluation of the Latest 40 Mile Model

In the rest of this document, we evaluate how well the latest version of the 40 mile model reproduces actual conditions in the river by comparing it to the first, calibrated version of the 40 mile model and to a variety of data sets.

Comparison to previous 40 mile model

In this section, we compare the latest version of the 40 mile model to the first version of the 40 mile model developed in 2013-2014. As described above, the main difference between the two models is that the new one has bands of much smaller (~2 ft. wide x ~10 ft. long) cells along the channel margins. This change was made to enable the new model to more faithfully reproduce the slow, shallow water along the channel margins that provides critical juvenile salmonid rearing habitat. The new model has 2,010,192 elements, more than twice as many as the previous model (898,656 elements). The additional elements significantly increased the computational costs, but also improved the model results. The differences between the two models are summarized in Table 3.

Table 3. Summary of differences between the original version of the 40 mile model and the latest version.

	1st version of 40 mile model **(also called the Habitat Model in some figure labels)**	**Latest version of 40 mile model** **(also called the Fish Production Model in some figure labels)**
Development Timeframe	Fall 2013 and Early 2014	Late 2014 - 2015
Motivation	Estimate the quantity and quality of salmonid habitat.	Improve estimates of salmonid habitat.
Number of Mesh Elements	898,656	2,010,192
Meshing Strategy	Uni-modal channel element size distribution	Bi-modal channel element size with smaller elements along the channel margins.
Roughness Assignment and Model Calibration	Calibrated by tuning the roughness to match observed water surface elevations. Floodplain roughness was uniform.	Roughness assigned from observations of sediment grain size, in-water cover, and floodplain vegetation and then compared to the previous, calibrated version of the model.

Comparison of water surface elevation residuals along a long profile

Figure 6 shows the differences in water surface elevation between the two versions of the model along the entire 40 mile long-profile at dam releases up to 11,000 cfs. Figure 7 shows the differences for the tributary accretion runs. At lower flows, the median water surface residual is less than about +0.1 ft., meaning that the new model is slightly deeper, as should be expected if the new model contains more

slow water at the same discharge. At higher flows, the new model becomes progressively deeper relative to the previous one. At 11,000 cfs, the median misfit is about 0.4 ft. However, the previous model was calibrated primarily to water surface elevation observations at flows lower than 4500 cfs, so it is entirely possible that it is inaccurate for the highest flows. It should also be noted that if the model misfit was expressed as a fraction of the water depth, the misfit at higher flows would likely be smaller.

The tributary accretion flows show a similar pattern. The median residual for all tributary accretion cases is less than 0.1 ft.

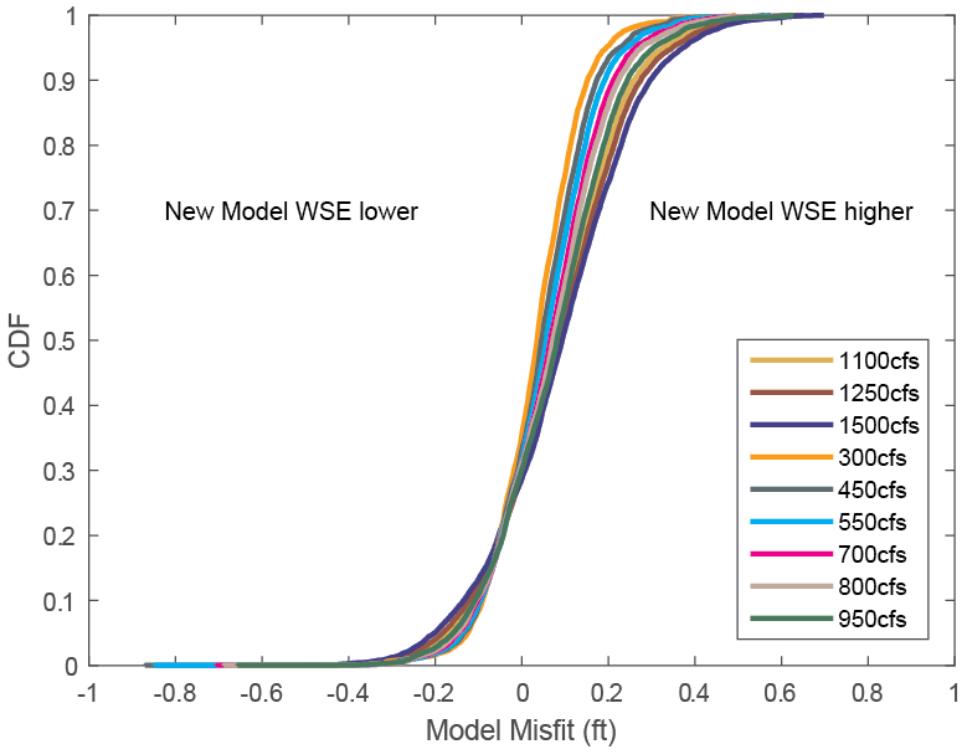

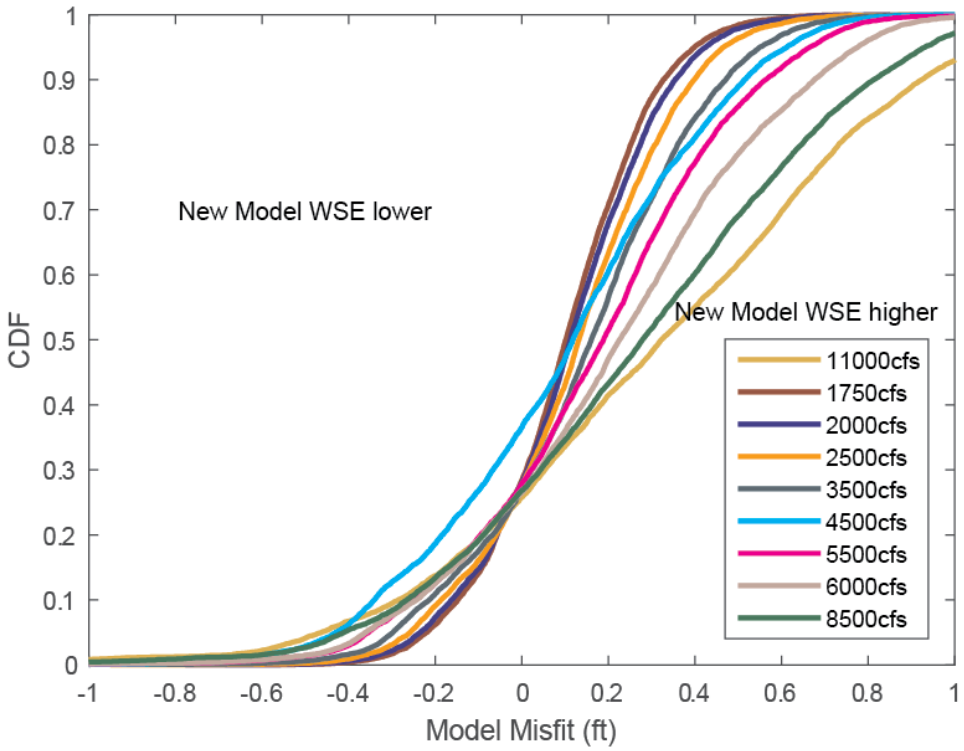

Figure 6. Water surface elevation residuals for flows between 300 cfs and 1500 cfs (top) and flows between 1750 cfs and 11,000 cfs (bottom). The new model water surface is slightly higher than the previous model and the misfit increases with increasing flows. For lower flows, the median difference between the new model the previous 40 mile model is about 0.1 ft. For the highest flows, the median difference increases to about 0.4 ft.

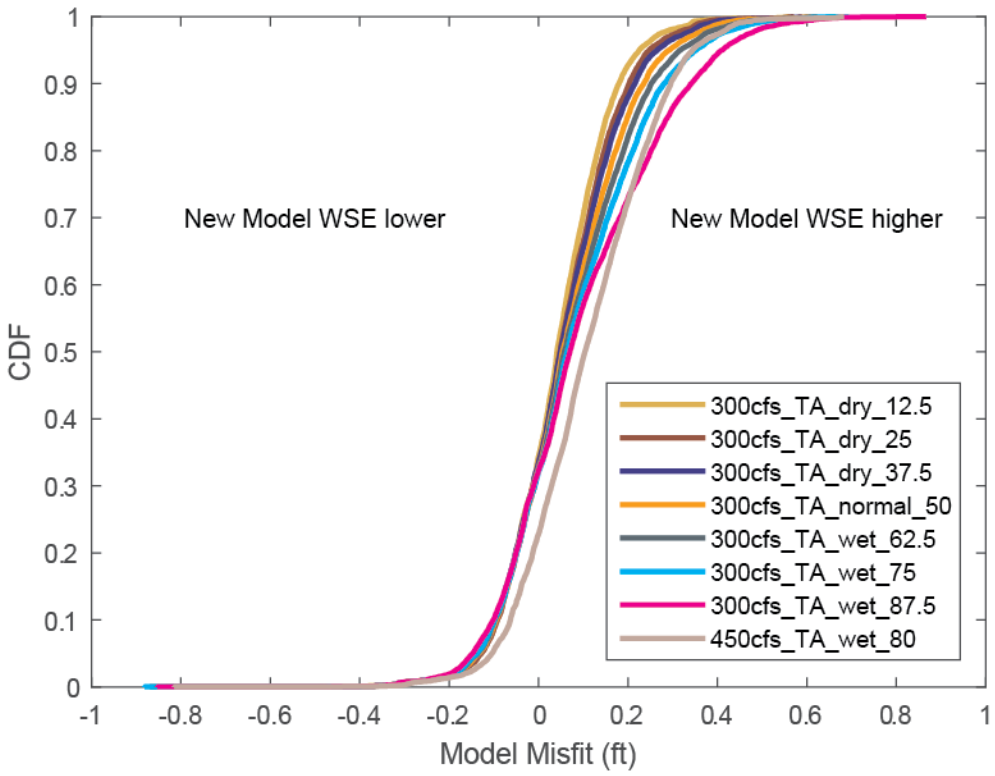

Figure 7. Water surface elevation residuals for the tributary accretion flows. The median difference between the new model and the previous 40 mile model is less than 0.1 ft. for all flows. Tributary accretion flows are described in Appendix A.

Comparison of depth distributions

Figure 8, Figure 9, and Figure 10 show comparisons of the two models' water depth probability distributions computed as the fraction of area shallower than a particular value for the dam release flows. Figure 11 and Figure 13 show the same comparison for the tributary accretions flows. At less-than-bankfull flows (up to 3500 cfs), the new model is uniformly deeper by a few inches than the old one. At higher flows, 4500 cfs and up, where the floodplain starts to engage, the new model shows an increase in the area occupied by shallow water (less than about 5 feet deep) of ~1-10% for a given depth over the previous model. This is partially due to the fact that the new model is deeper at higher flows than the previous model. Better representation of the changes in surface elevation by the smaller mesh elements along the channel margins may also play a role.

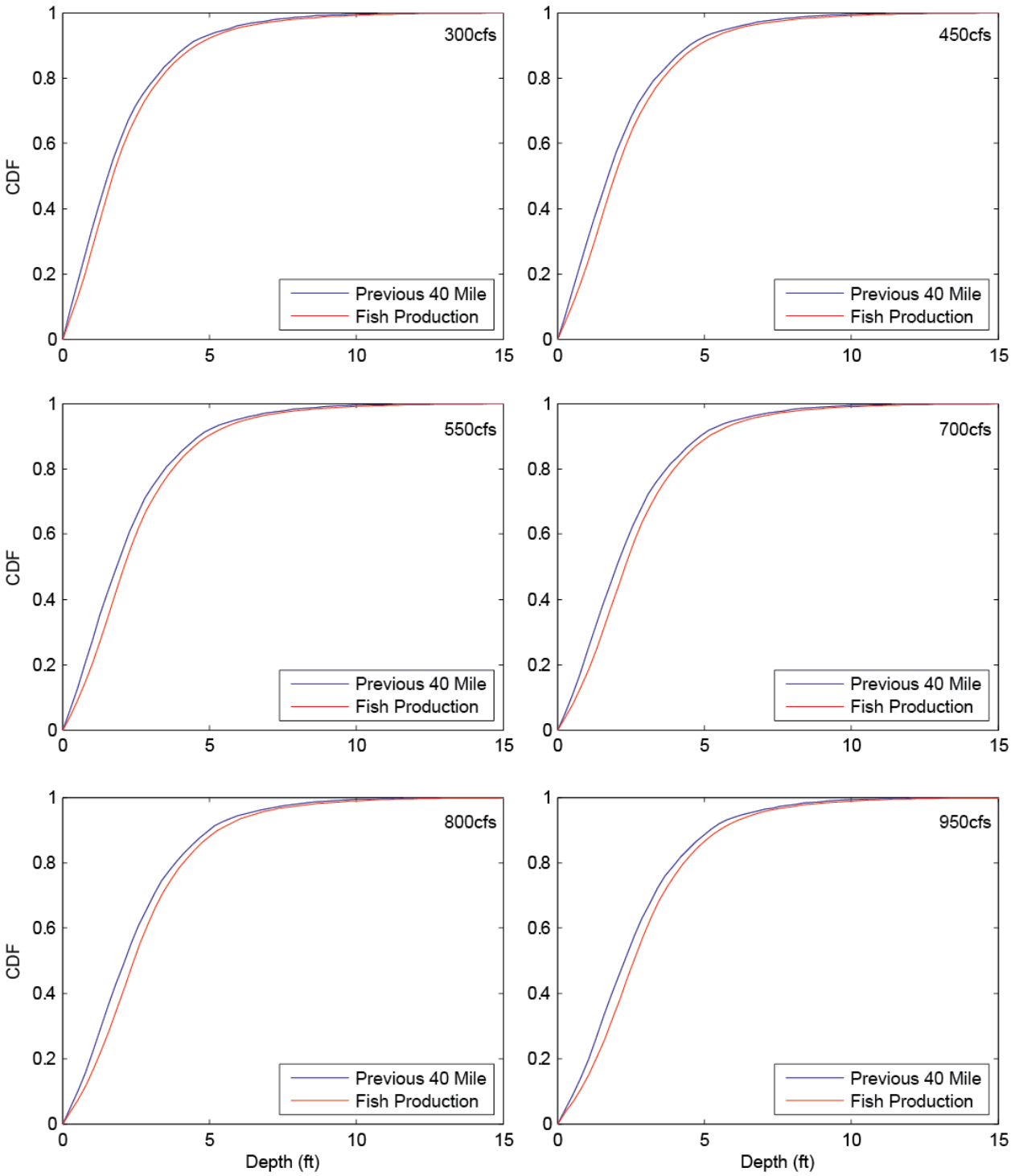

Figure 8. Area-weighted distributions of water depth for flows from 300 cfs to 950 cfs. The latest version of the model is a few inches deeper than the previous 40 mile model.

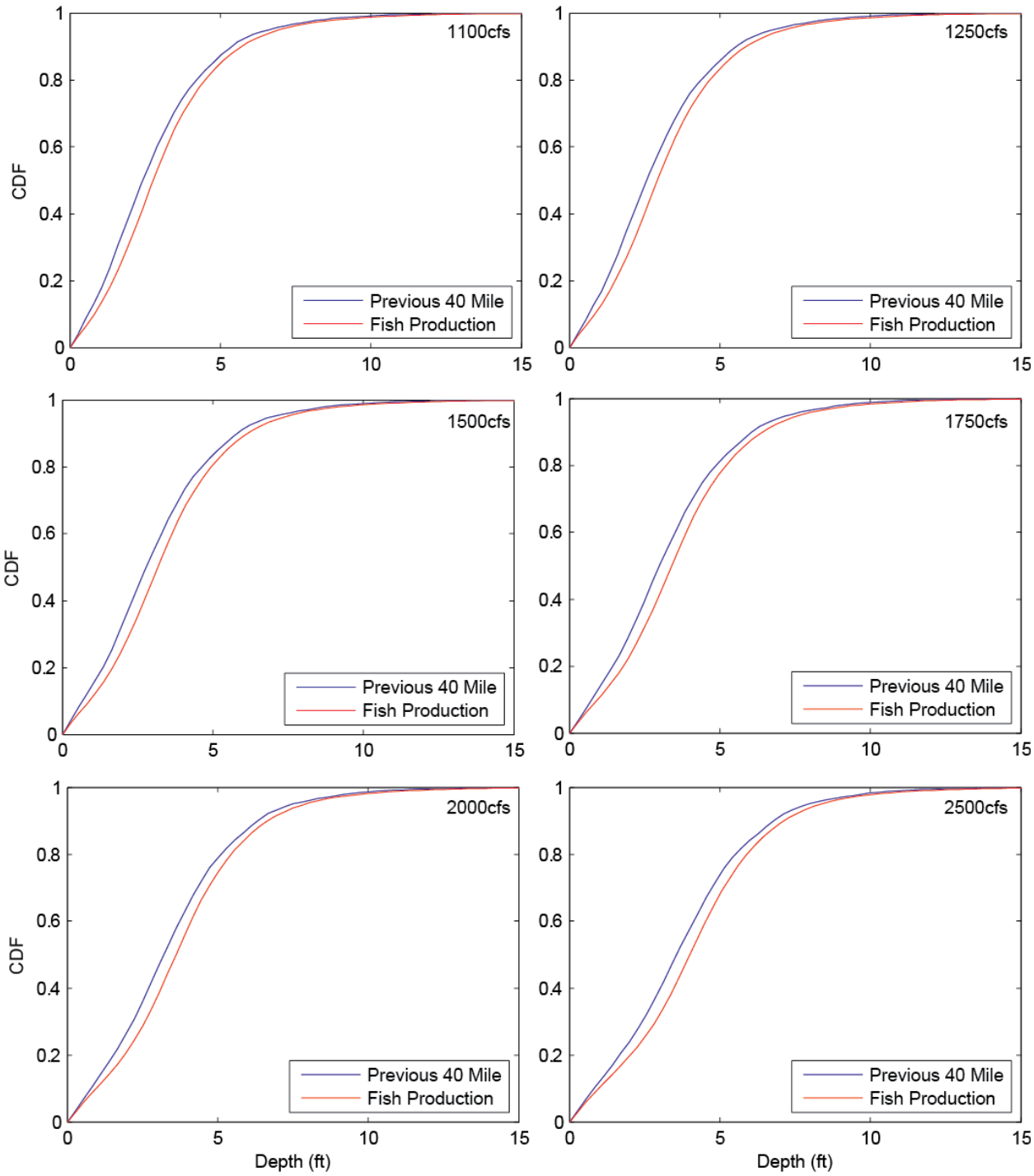

Figure 9. Area-weighted distributions of water depth for flows from 1100 cfs to 2500 cfs. The latest version model is a few inches deeper than the previous 40 mile model.

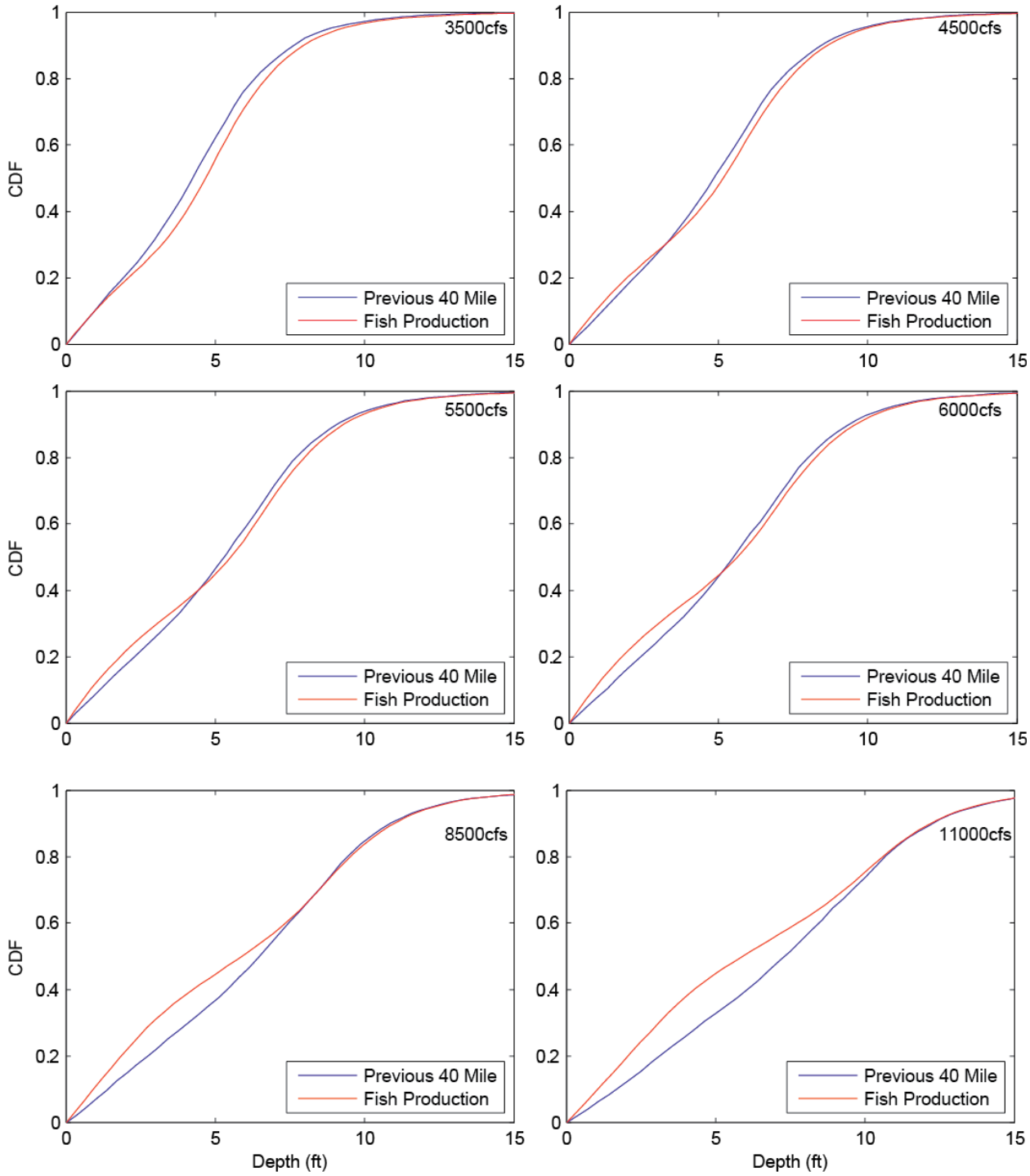

Figure 10. Area-weighted distributions of water depth for flows from 3500 cfs to 11,000 cfs. The latest version of the model shows an increase in area occupied by shallow water at flows higher than bankfull (3500 cfs and above). For a given depth, the increase ranges from about 1-10%.

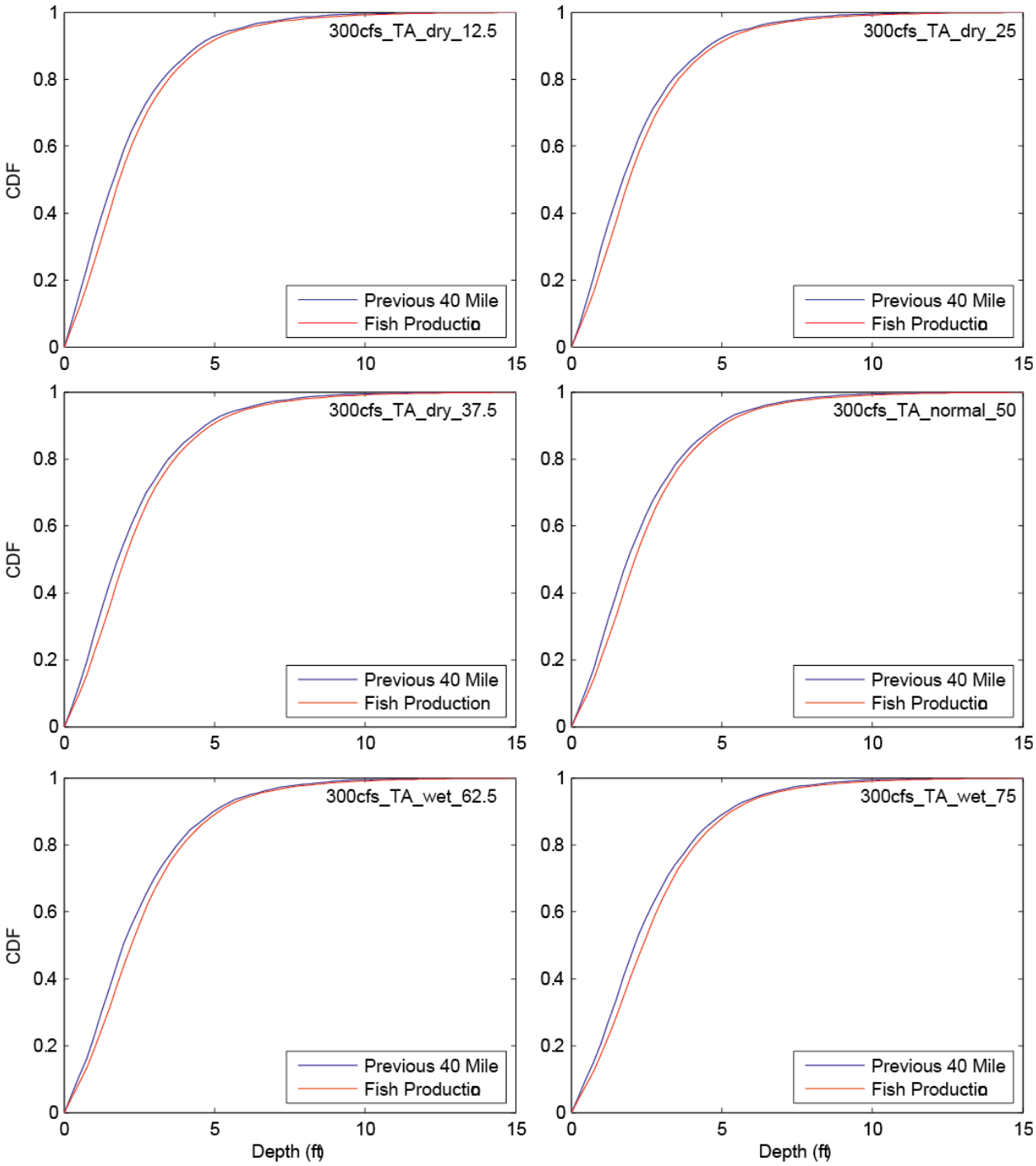

Figure 11. Area-weighted distributions of water depth for the 300 cfs tributary accretion flows. The latest version of the model is a few inches deeper.

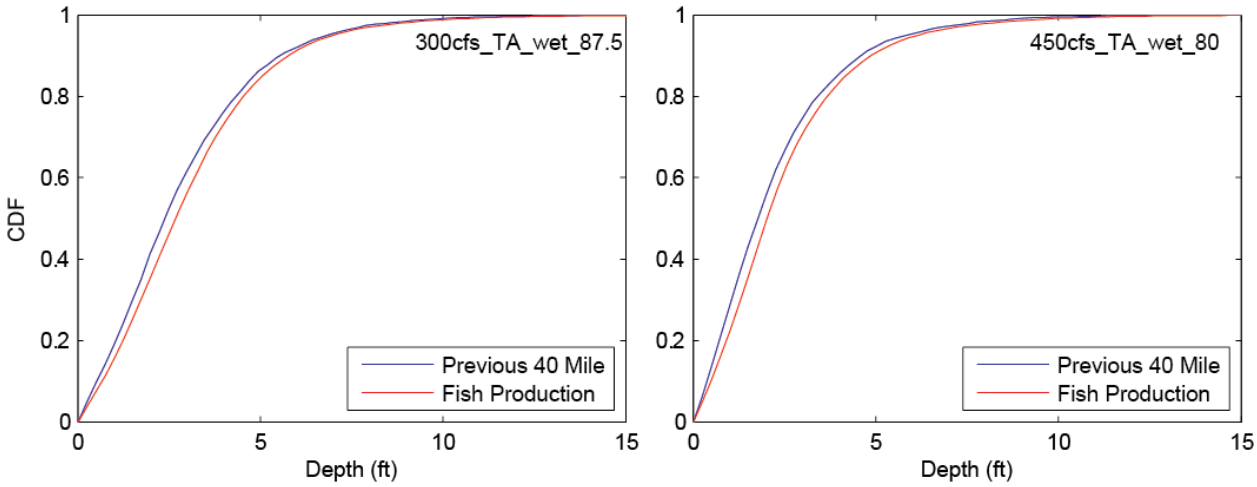

Figure 12. Area-weighted distributions of water depth for the highest 300 cfs tributary accretion flow and the 450 cfs tributary accretion flows. The latest version of the model is slightly deeper.

Comparison of velocity distributions

Figure 13, Figure 14, and Figure 15 show comparisons of the two models' flow velocity probability distribution computed as the fraction of area slower than a particular value for the dam release flows. Figure 16 and Figure 17 show the same comparison for the tributary accretions flows. The new model has more area with slow water than the previous model at all flows. At lower flows, up to 2500 cfs, the fraction of water slower than about 3 ft./s is about the same in both versions of the model. In areas of the river with higher velocities, the new model is slightly slower (one to a few 0.1 ft./s). At higher flows (3500 cfs and above), there is more slow water everywhere. For example, at 5500 cfs, about 15% of the area in the new version of the model is slower than 1 ft./s. In the previous version, less than 10% of the area was less than 1 ft./s. At this flow, the new model shows an approximate 5% increase in the amount area with optimal velocity for pre-smolt salmonids.

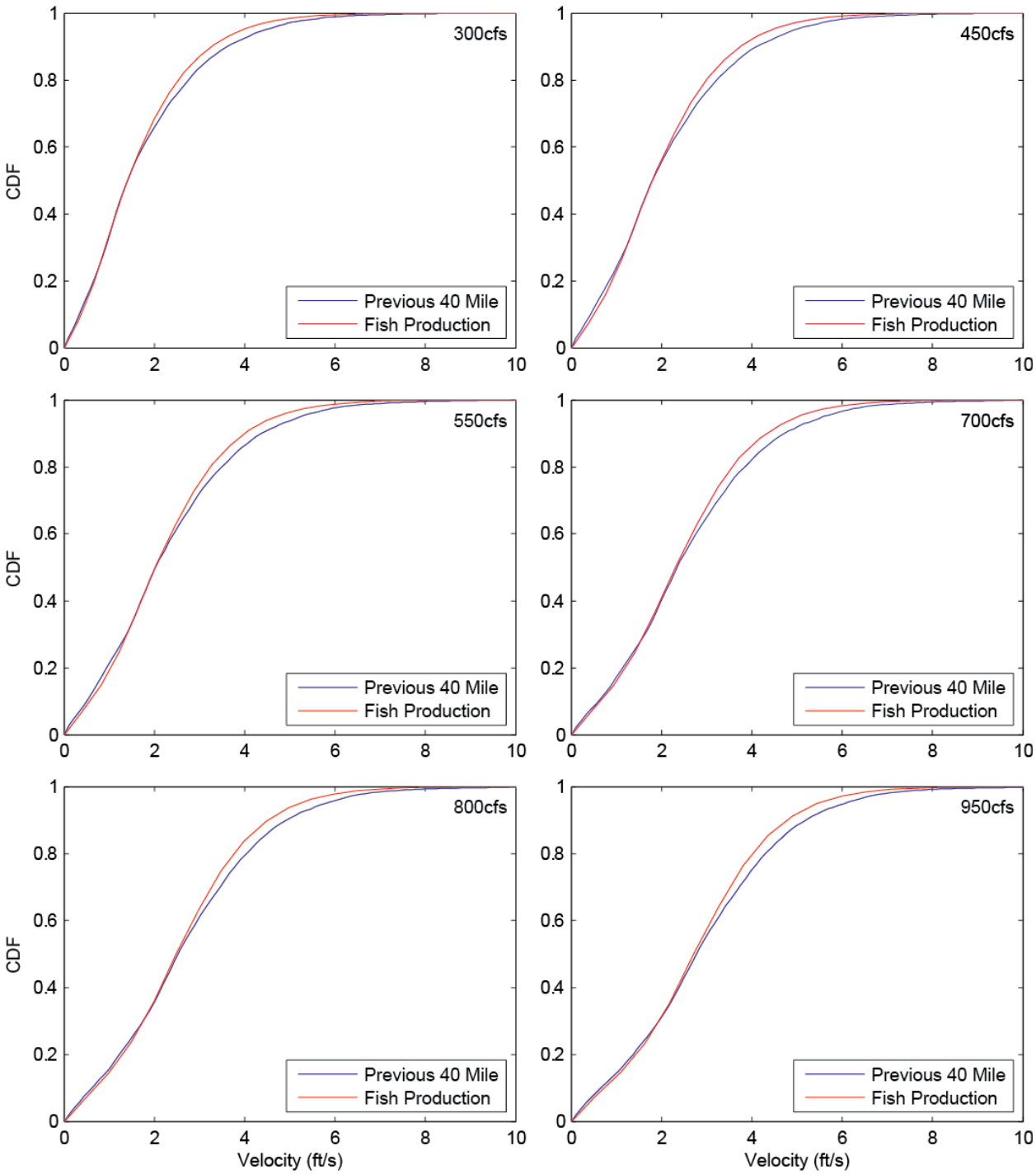

Figure 13. Area-weighted distributions of water velocity for flows from 300 cfs to 950 cfs. The fastest 40-50% of wetted area in the latest version of the model is slightly slower than in the previous 40 mile model.

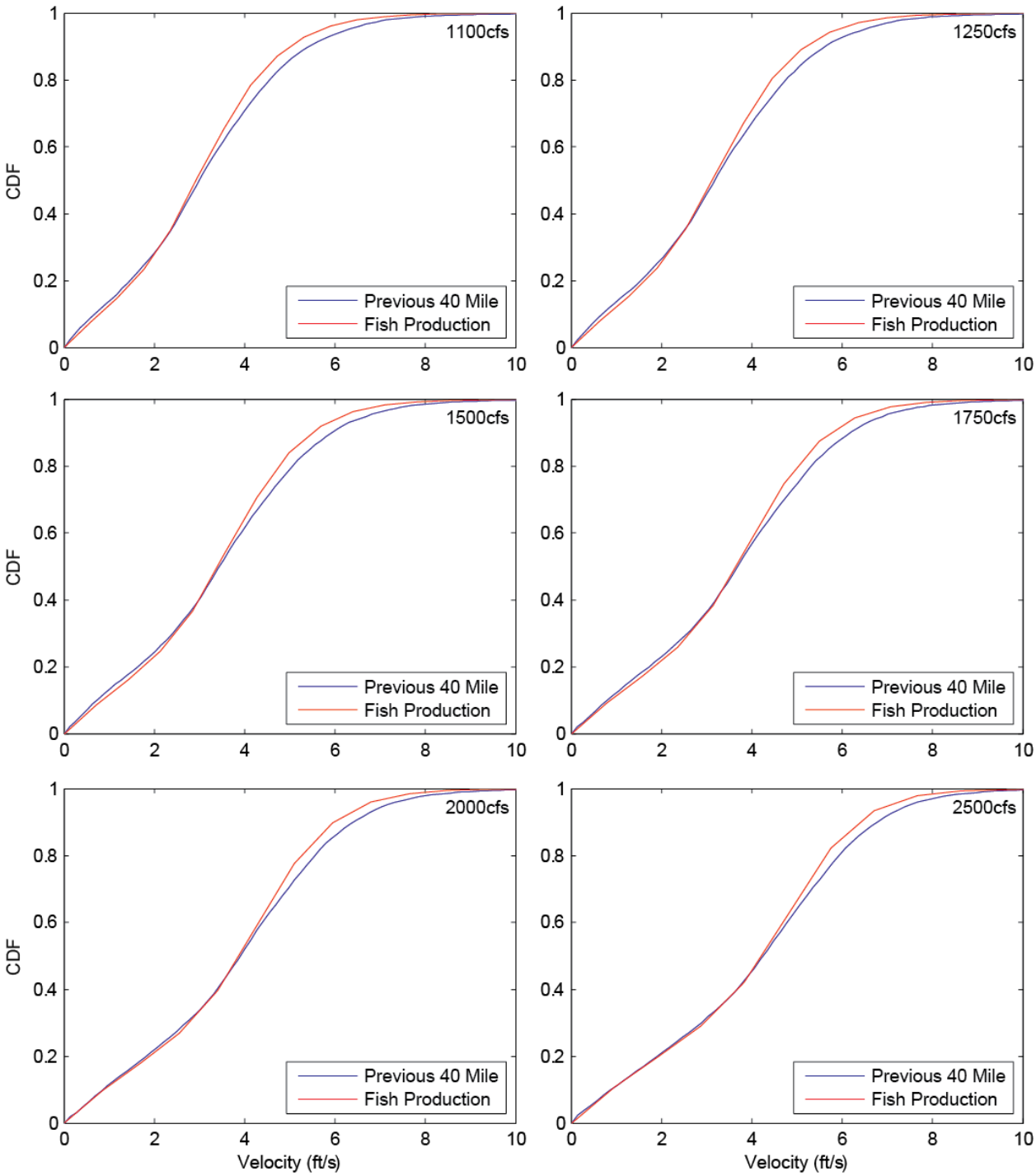

Figure 14. Area-weighted distributions of water velocity for flows from 1100 cfs to 2500 cfs. The fastest 40-50% of wetted area in the latest version of the model is slightly slower than in the previous 40 mile model.

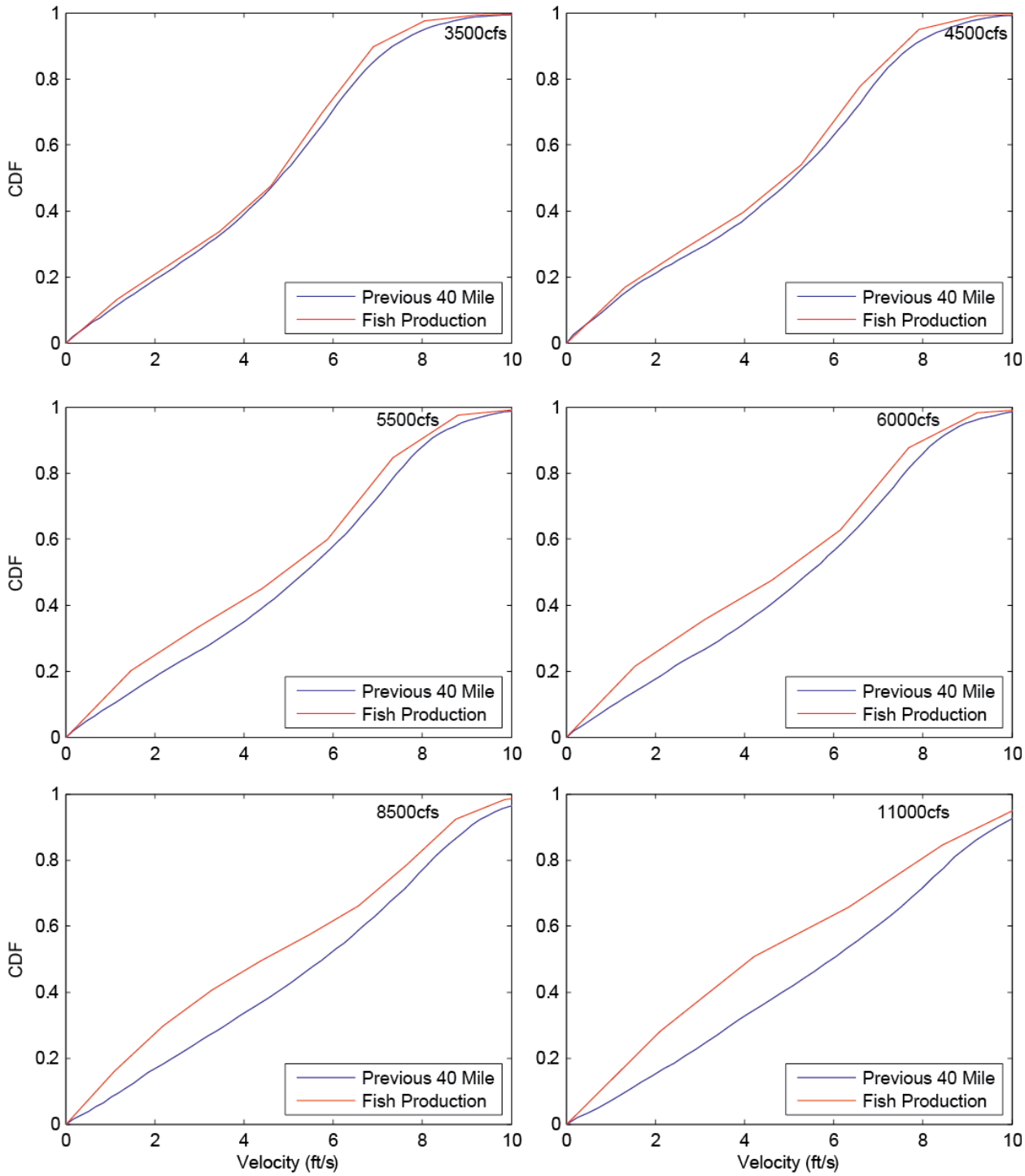

Figure 15. Area-weighted distributions of water velocity for flows from 3500 cfs to 11,000 cfs. The new version of the model is slower than the old one over nearly 100% of the wetted area and up to 2 ft./s slower at the highest flows. At flows of 5500 cfs and higher, the new model shows a 5-10% increase in the amount of area with velocities less than 1 ft./s, the approximate threshold velocity for optimal pre-smolt habitat.

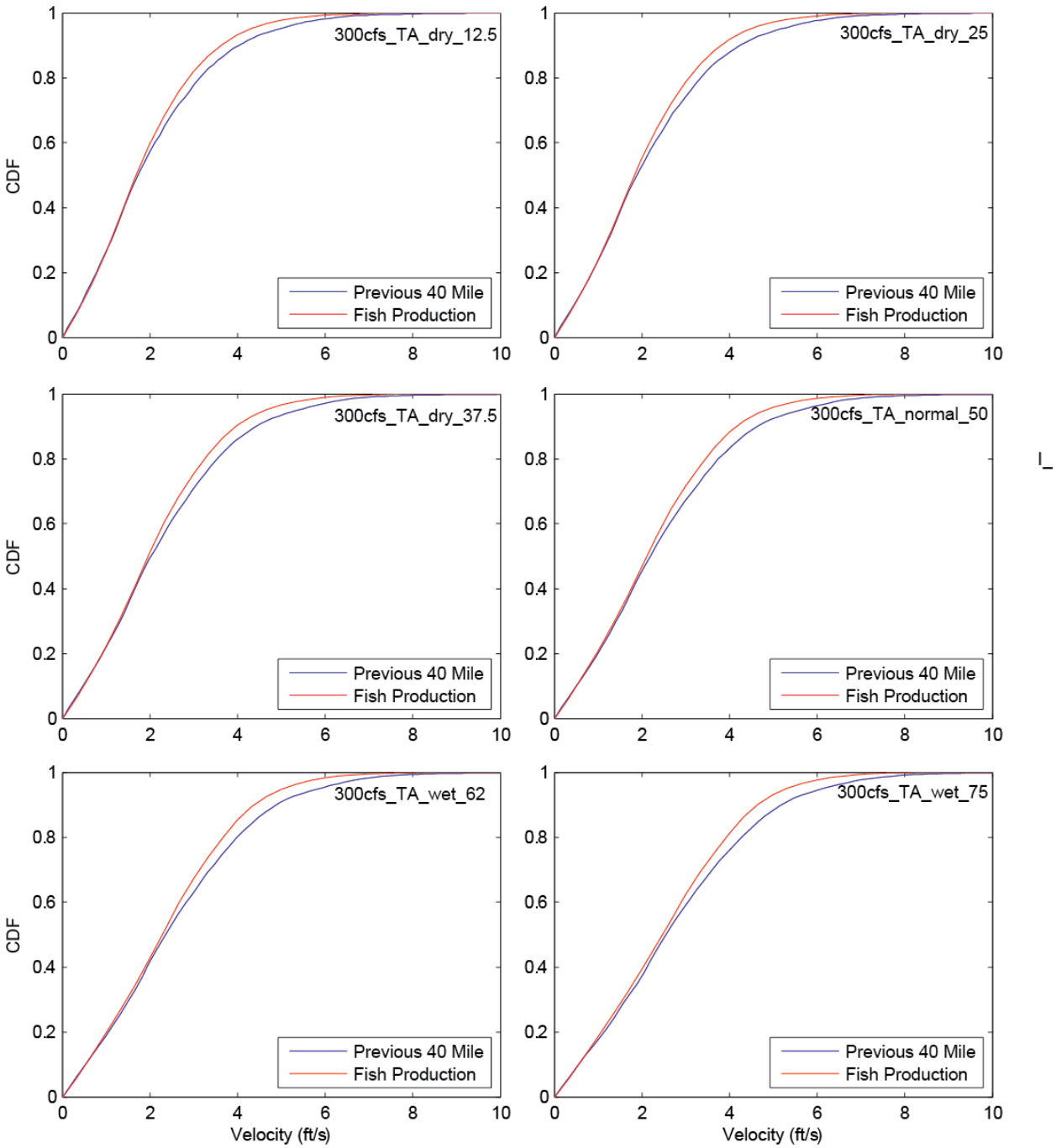

Figure 16. Area-weighted distributions of water velocity for the 300 cfs tributary accretion flows. The fastest 40-50% of water in the new version of the model is slightly slower than in the previous model.

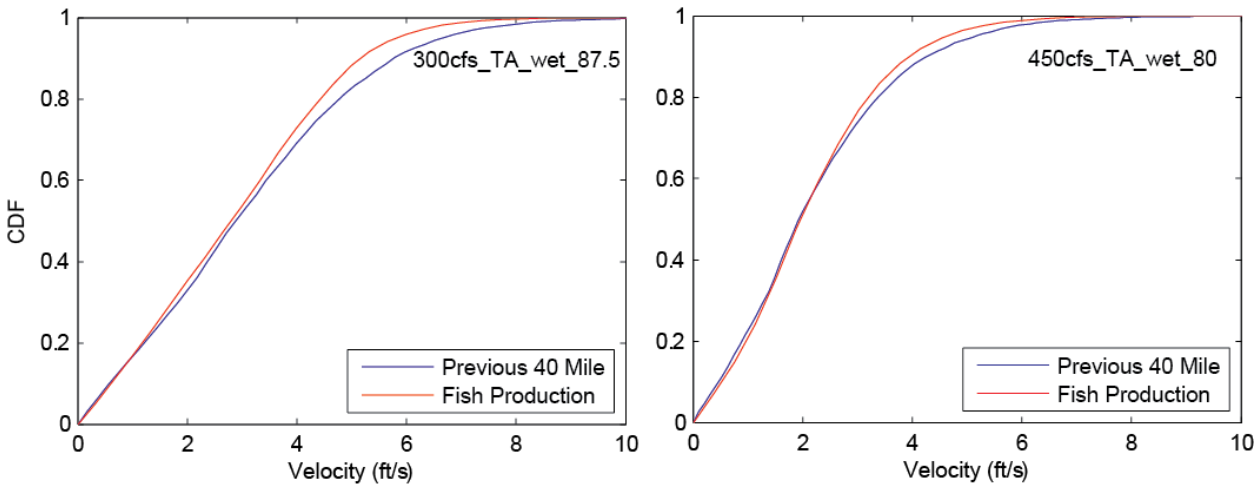

Figure 17. Area-weighted distributions of water velocity for the highest 300 cfs tributary accretion flows and the 450 cfs tributary accretion flow. The 300 cfs flow is slower than the previous version of the model over approximately 80% of the wetted area. The 450 cfs flow is slower than the previous version of the model over approximately 30% of the wetted area.

Comparison to water surface elevation and velocity observations

In this section, the new version of the 40 mile model is compared to observations of water surface elevation and flow velocity. The observations were made in 2010 at the Junction City Campground, Round House, Evans Bar, Sheridan, and Valdor Gulch. The velocity measurements are compared to the model flow that is most similar to the observed discharge when the measurement was taken.

Water Surface Elevation Comparison

Figure 18 shows a comparison of the model water surface elevation to observations of water surface elevation (WSE) made by Graham Matthews and Associates (GMA) during the bathymetric survey. We consider these the most appropriate water surface observations for comparison to the model because they were collected at the same time as the bathymetry used in the model. The observations were collected at a flow of approximately 4,300 cfs and are confined to the Dutch Creek to Oregon Gulch reach. They were part of the data set used in calibrating the first version of the 40 mile model. To compare the modeled and observed elevations, the observed elevation data set was linearly interpolated to the centers of the model cells.

The top panel shows observed WSE vs. modeled WSE at 4500 cfs. The slope of a mesh cell area weighted linear regression to the comparison is 1.01 with an area weighted R^2=0.997, but a non-zero intercept, indicating the new model is systematically higher than the observations. The bottom panel confirms this. It shows the mesh cell area weighted distribution of WSE residuals from the original version of the 40 mile model and from the new version of the model. The median misfit for the new version of the model is about 0.6 ft. too high. The median misfit for the previous model is less than 0.1 ft., which is unsurprising since it was calibrated to these observations.

Figure 19 shows a comparison of the 3500 cfs model water surface compared to WSE observations collected in Sept. 2014 at a flow of 3400 cfs. The pattern of misfit is nearly identical to the previous comparison. The new version of the model is higher, with a median misfit of approximately 0.5 ft. Because of the way the comparison was performed, cell area is not taken into account in the regression and when constructing the CDF, so this should be considered an approximate median misfit. It would likely change by a small amount if cell area were taken into account when constructing the cumulative distribution.

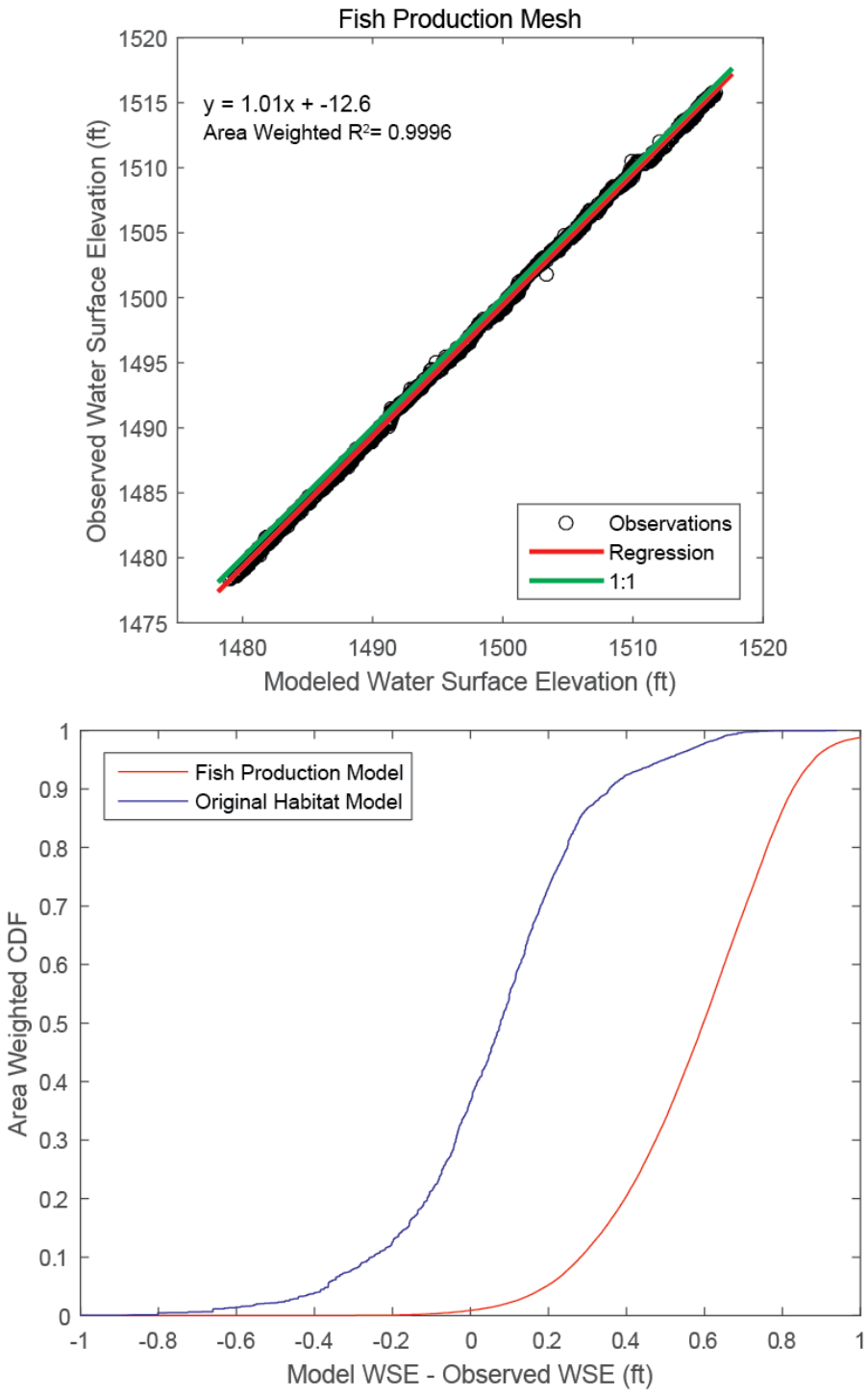

Figure 18. The model at 4500 cfs compared to water surface elevations collected by GMA during the bathymetry survey. Flows during most of the survey ranged between 4200 and 4300 cfs. The top plot shows that there is excellent correlation between the observed and modeled water surface in the latest version of the model, but the model water surface is slightly higher. The bottom plot shows that the median elevation residual is about 0.6 ft. The apparent inconsistency with Figure 6, which shows that the new model is about 0.1 ft higher than the previous 40 mile model at 4500 cfs, is likely due to the fact that the observations in this figure are confined to the Dutch Creek to Oregon Gulch reach, while Figure 6 compares the models along the entire 40 miles. A second difference is that Figure 3 compares models along a 1D long profile as opposed to the 2D comparison shown here.

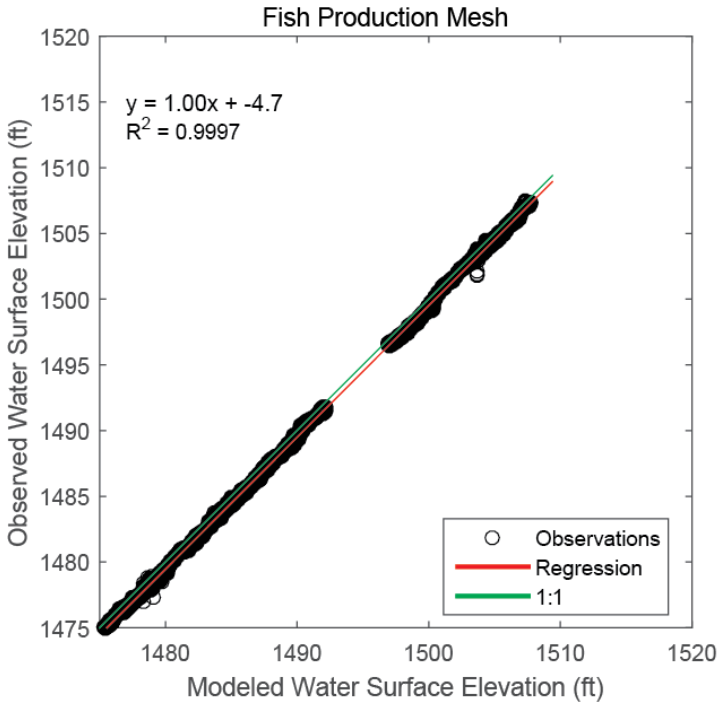

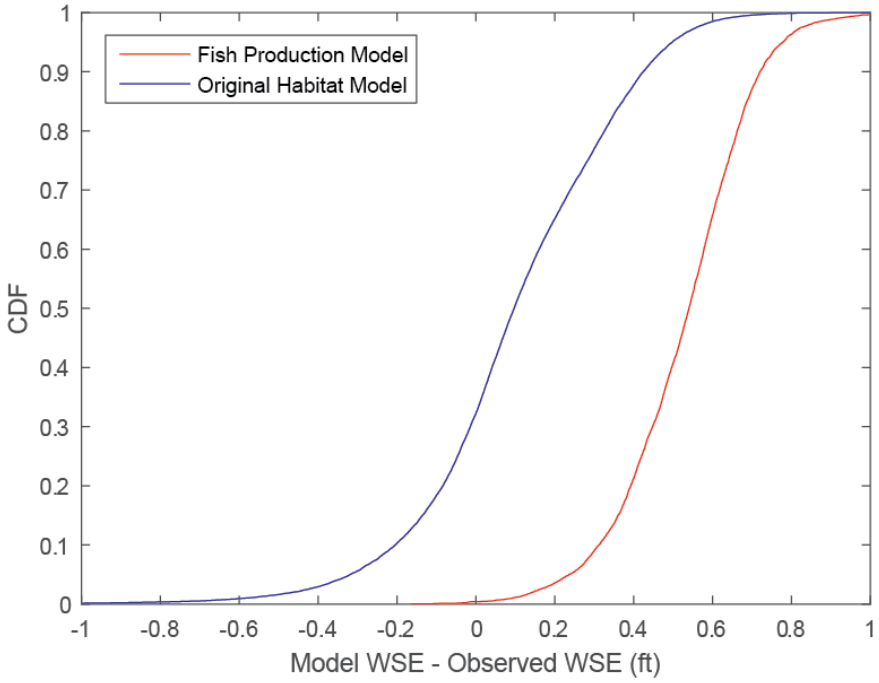

Figure 19.The latest version of the 3500 cfs model water surface elevations compared to observations collected at 3400 cfs in Sept. 2014. There is excellent correlation (top panel), but the new model water surface is about 0.5 ft higher than the observations and the previous 40 mile model. The apparent inconsistency with Figure 6, which shows that the new model is about 0.3 ft higher than the previous 40 mile model at 3500 cfs, is likely due to the fact that the observations in this figure are confined to the Evans Bar to Oregon Gulch reach, while Figure 6 compares the models along the entire 40 miles. A second difference is that Figure 3 compares models along a 1D long profile as opposed to the 2D comparison shown here.

Velocity Comparison

Figure 20 shows the comparison of the latest version of the model to point velocity measurements collected at Evans Bar, Round House, Sheridan, Valdor Gulch, and the Junction City campground at flows ranging from 530 cfs to 6500 cfs. Data from the first version of the model are not included in the analysis. The observations are compared to the model flow that is most similar. The comparison algorithm examines model velocities at all model cells within 6 feet of the location of the observation and selects the model cell with the smallest velocity residual as the basis for comparison. The top panel shows observed velocity plotted vs. model velocity for all flows. The linear regression (red line) has a slope of 0.8 with a mesh cell area weighted $R^2 = 0.64$. This indicates that the latest version of the model is on average faster than the observations it is compared to. However, a number of points fall very close the 1:1 line (black line). Many of the points that fall far from the 1:1 line are very low or negative observed velocities. Higher velocities tend to fall closer to the 1:1 line. The bottom panel shows the mesh cell area weighted probability distribution of velocity residuals. The median misfit is much less than +/- 1 ft./s for all flows, but more than 50% of the comparisons result in a model velocity that is higher than the observed.

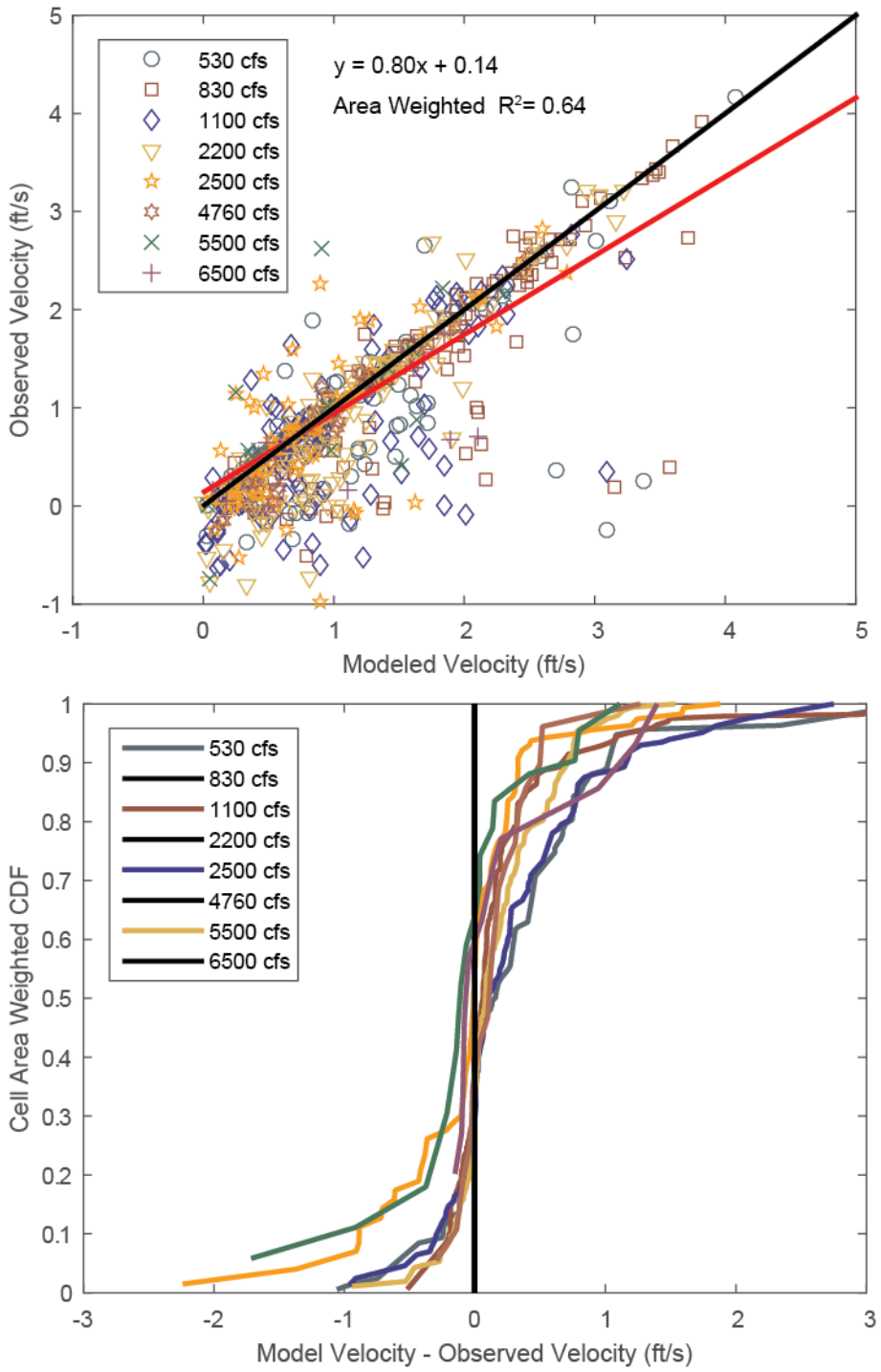

Figure 20. Water velocity from the latest version of the model compared to point velocity measurements. The observed velocities are compared to model velocities at the model flow that is most similar (e.g. 500 cfs model compared to the 530 cfs observations). The observations are compared to the model velocity within a 6 foot radius that is the most similar. The top plot shows that the regression to all the comparisons (red line) has a slope less than 1, indicating that on average, the model water is faster than the observations. However, many observations fall on or near the 1:1 line (black line). The bottom plot shows that the median velocity residual for all flows is less than +/- 1 ft./s at all flows, but generally biased positive, indicating that model water is faster than the observations.

Comparison to Observed Habitat

In this section, the amount and type of modeled habitat from the latest version of the 40 mile model is compared to habitat observations. Only pre-smolt habitat is shown. Fry habitat shows similar patterns, but with less area. The habitat observations are derived from the layer Trinity_River_Habitat_Assessment/GRTS_HabitatArea intersected with a generalized random tessellation stratified (GRTS) panel layer to add the GRTS panel ID to the habitat polygons. The subset of these observations used in the comparison is summarized in in Table 4.

Table 4. Summary of categorical habitat observations

Year	Minimum Discharge (cfs)	Maximum Discharge (cfs)	Number of Observations	Restricted Discharge Range (cfs)	Number of Observations.	Mean Observed Discharge (cfs)	Model Discharge (cfs)
2009	393	501	44567	400-500	38,554	455	450
2010	443	596	45414	400-500 500-600	11,920 33,494	464 522	450 550
2011	439	603	46064	400-500 500-600	22,851 22,206	464 546	450 550
2012	430	593	45486	400-500	37,915	458	450
2013	440	507	49366	400-500	44,371	460	450

Habitat Area Comparison

The observed and modeled habitat area were summed over each GRTS panel. These sums were totaled to produce the bar charts of total habitat in each category. The categories are 1) Optimal depth and velocity but no cover (DV, No C), 2) Depth and/or velocity thresholds exceeded, but cover present (No DV, C), and 3) Optimal depth, velocity, and cover present (DVC). The probability distributions shown are computed over all panels that contain observations (Figure 21).

The model under-predicts the amount of habitat with optimal velocity because the model velocities are higher than the observed velocities. This results in too little area in the DV, No C category and too much area in the No DV, C category.

The model does not agree well with the 2009 and 2010 observations. However, a consistent pattern is apparent in the comparisons to the 2011, 2012, and 2013 observations. In general, the modeled DV, No C category has about 60% as much habitat area as observed and the No DV, C category has about 1.5x as

much area as observed. The total amount of cover in the model (No DV, C + DVC) is similar to the amount observed in 2011, 2012, and 2013.

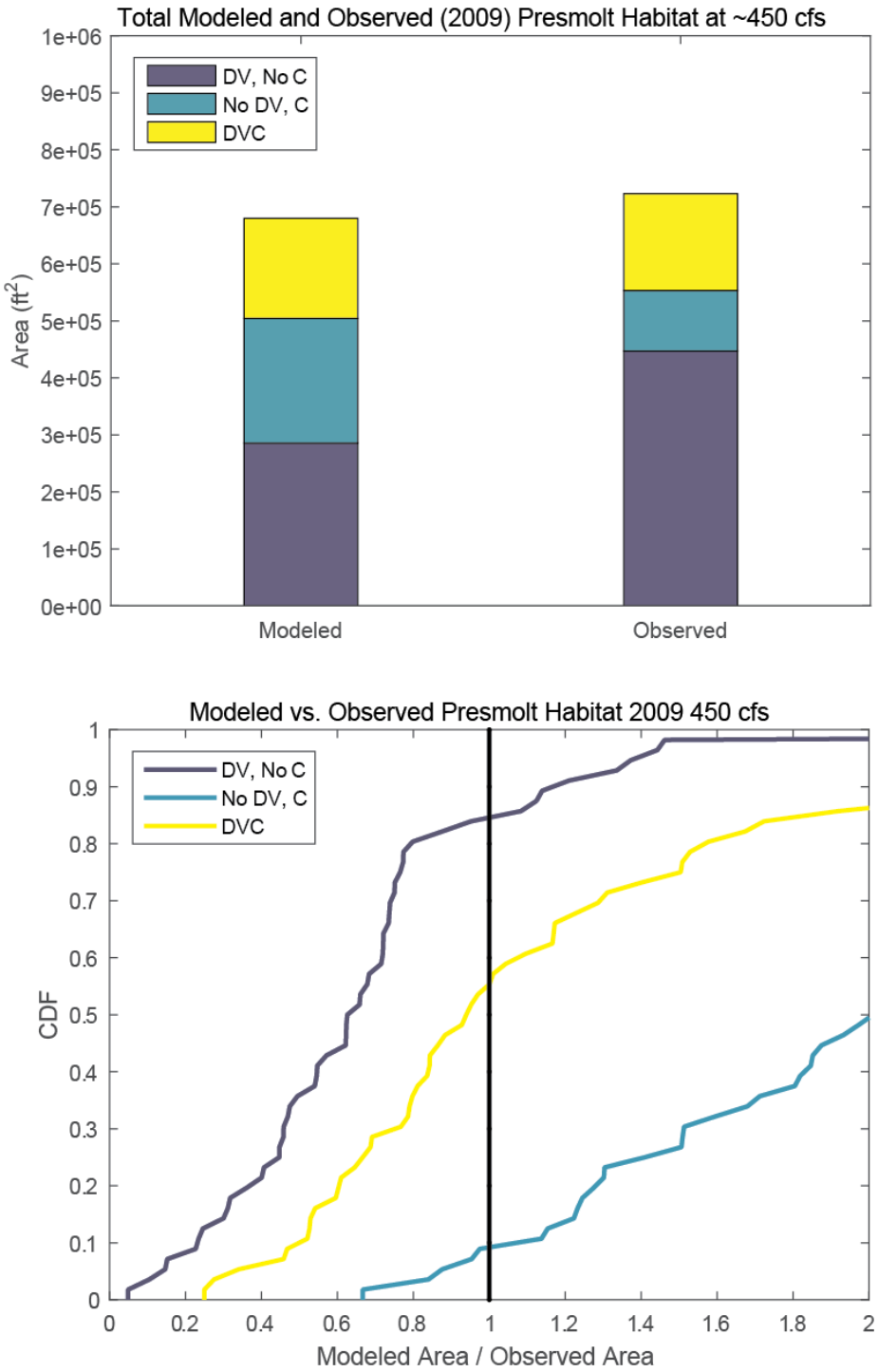

Figure 21. The latest version of the model at 450 cfs compared to 2009 habitat observations. The top plot shows habitat summed over all GRTS panels for which there are observations. The model under-predicts the amount of area in the DV, No C category and over-predicts the amount in the No DV, C category. The area in the modeled and observed DVC category is similar. The bottom plot shows the cumulative distribution of the ratio of modeled area to observed area over all the panels with observations. The DV, No C curve shows that the model underestimates the amount of habitat in that category in ~80% of the panels with observations. The model over-estimates the amount of habitat in the No DV, C category in about 90% of the panels. The DVC ratio is distributed approximately uniformly with a median near 1.

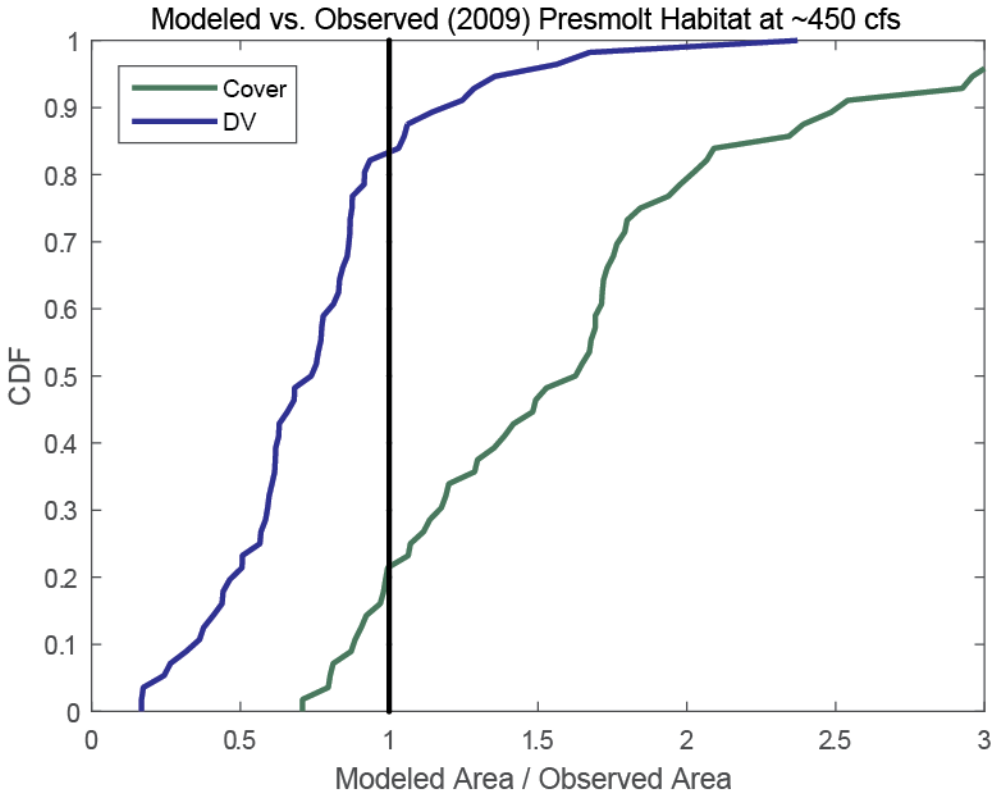

Figure 22. The distribution of the ratio of modeled to observed 2009 450 cfs habitat in the optimal depth and velocity categories (DV, No C + DVC) and the cover categories (No DV, C + DVC). The model under-estimates DV habitat in ~80% of the panels and overestimates the amount of cover in ~80% of panels. The median ratio of DV habitat is about 0.6, similar to other years. The cover ratio is larger than other years.

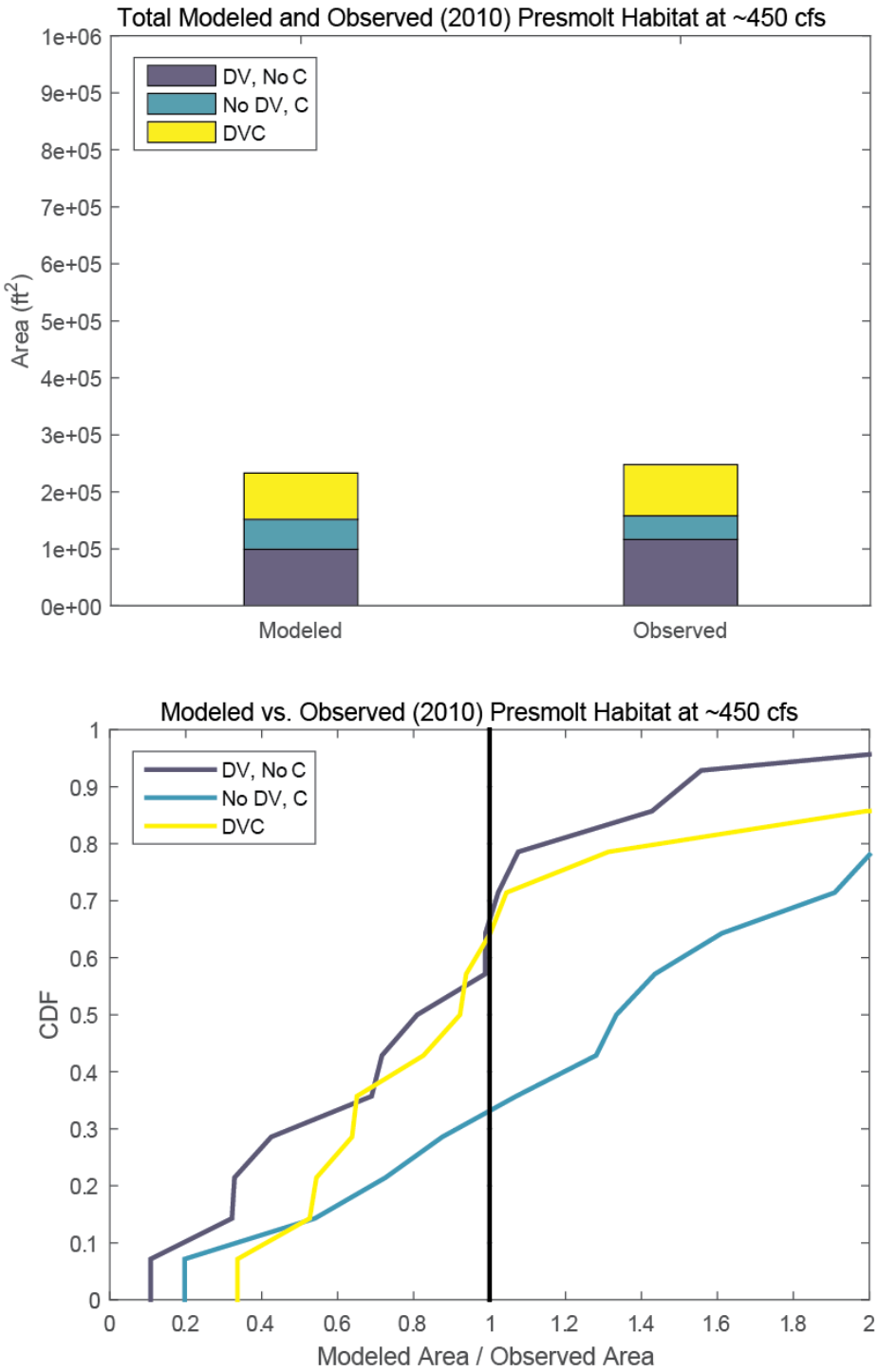

Figure 23. Comparison of the 450 cfs model compared to the 2010 450 cfs habitat observations. The model is similar to the observations in all categories. Optimal depth and velocity (DV) is underestimated by about 25-30% (the median of the DV, No C curve is about 0.75 and the median of the No DV, C curve is about 1.4. 1/1.4 = 0.71.) The median cover ratio is about 0.9.

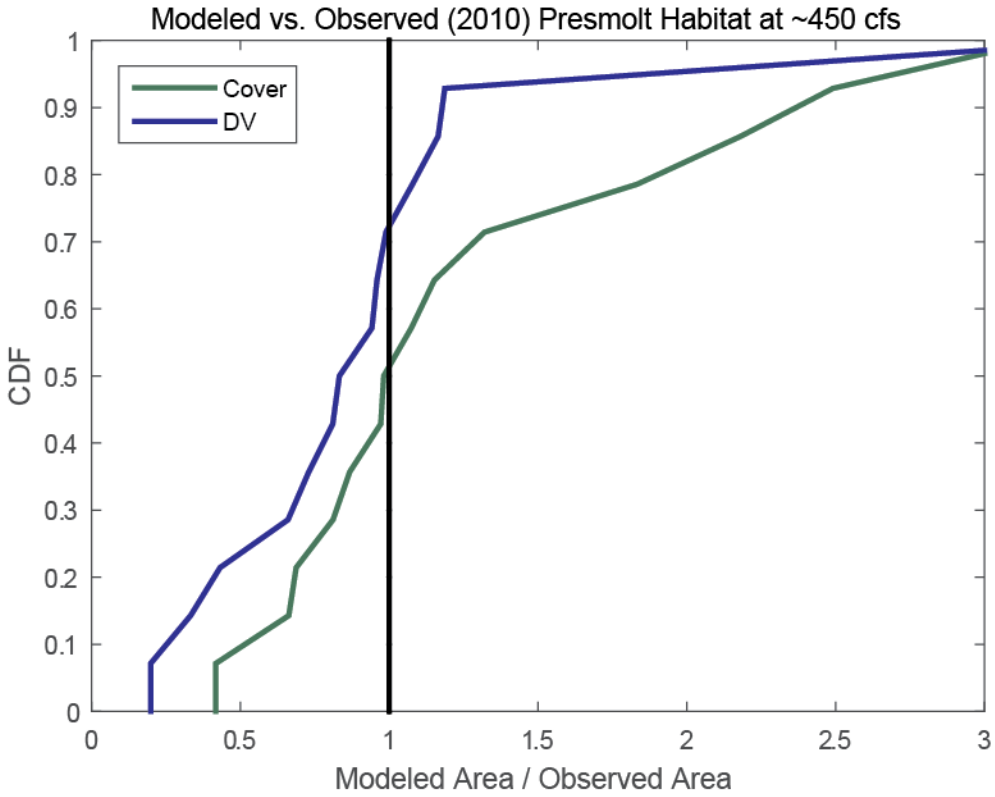

Figure 24. The distribution of the ratio of modeled to observed 2010 450 cfs habitat in the optimal depth and velocity categories (DV, No C + DVC) and the cover categories (No DV, C + DVC). The median ratio of DV area is about 0.8, consistent with the values in Figure 23. The median ratio of the cover area is close to 1.

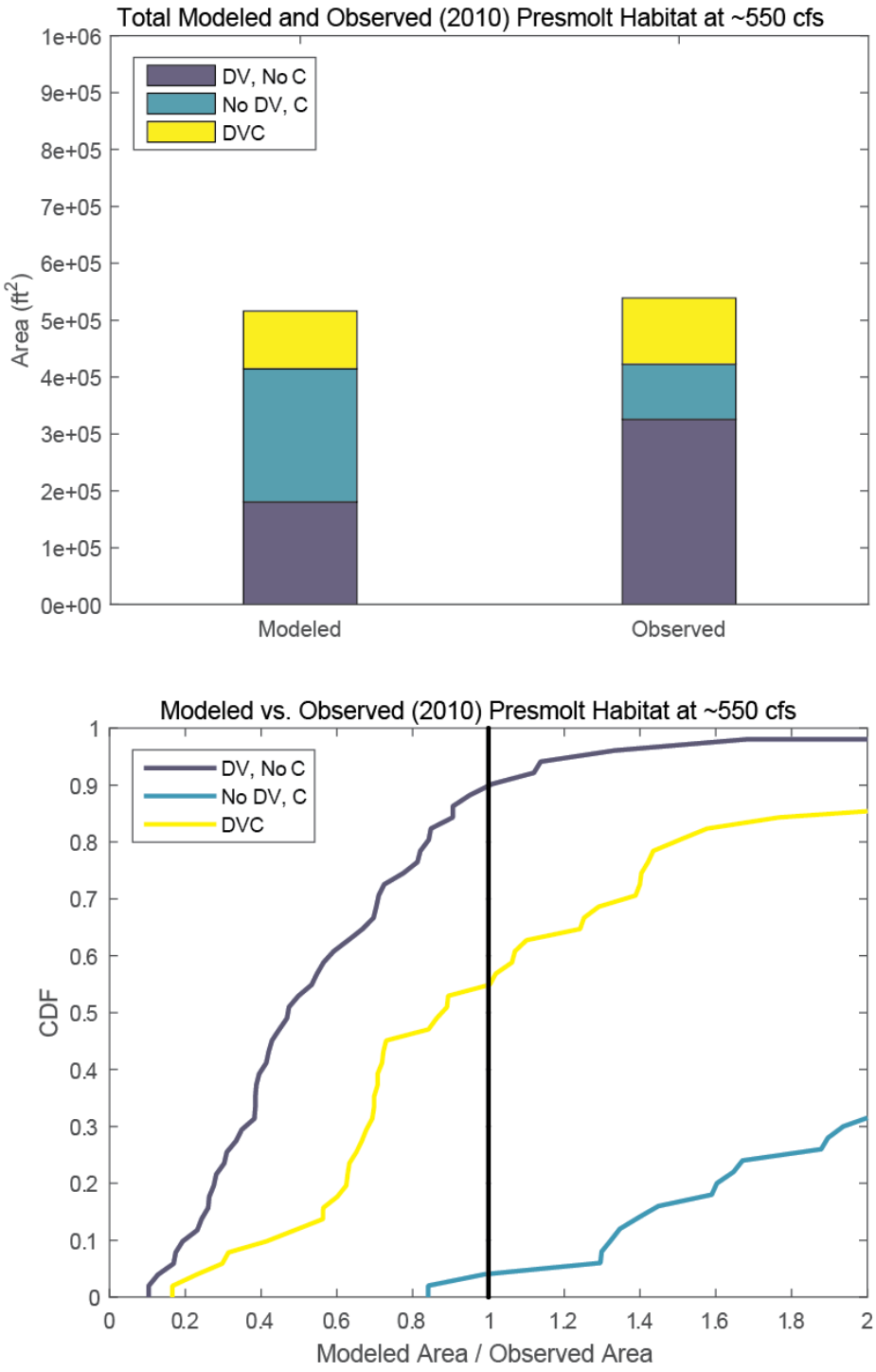

Figure 25. Comparison of the 550 cfs model to the 2010 522 cfs observations. The modeled area is similar to the observed area in the DVC category, but off by about a factor of 2 in the other categories.

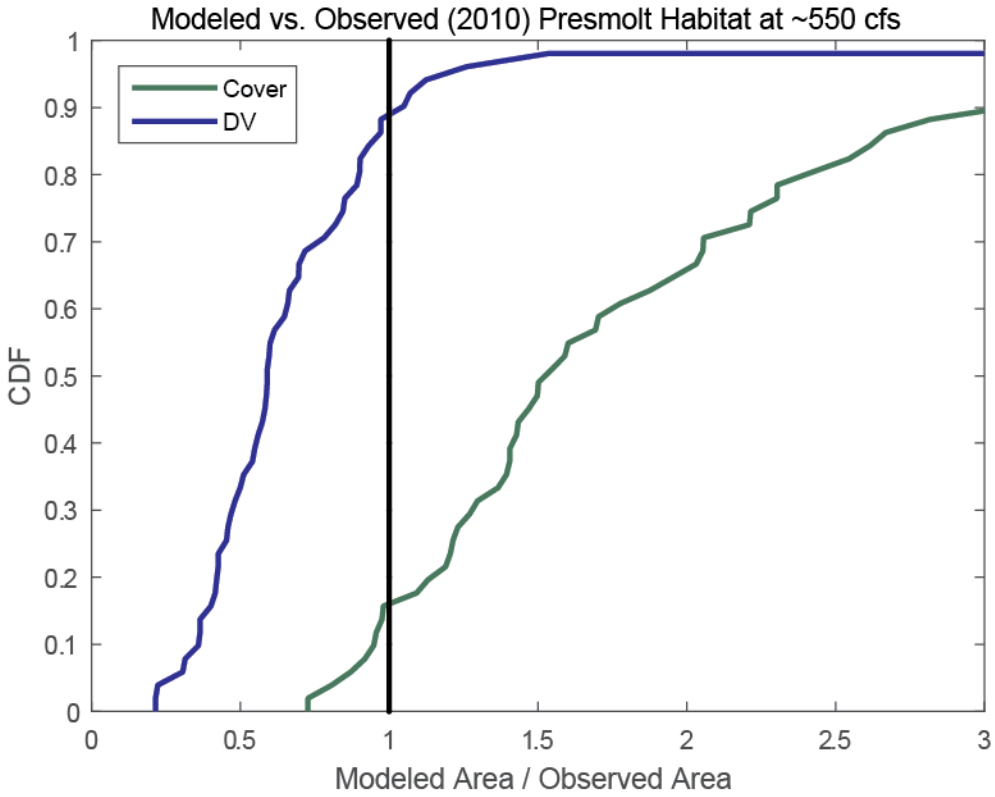

Figure 26. The distribution of the ratio of modeled area in the DV and Cover categories to the observed area. The model underestimates the amount of DV habitat in 90% of the panels and over estimates the amount of cover in 85% of the panels.

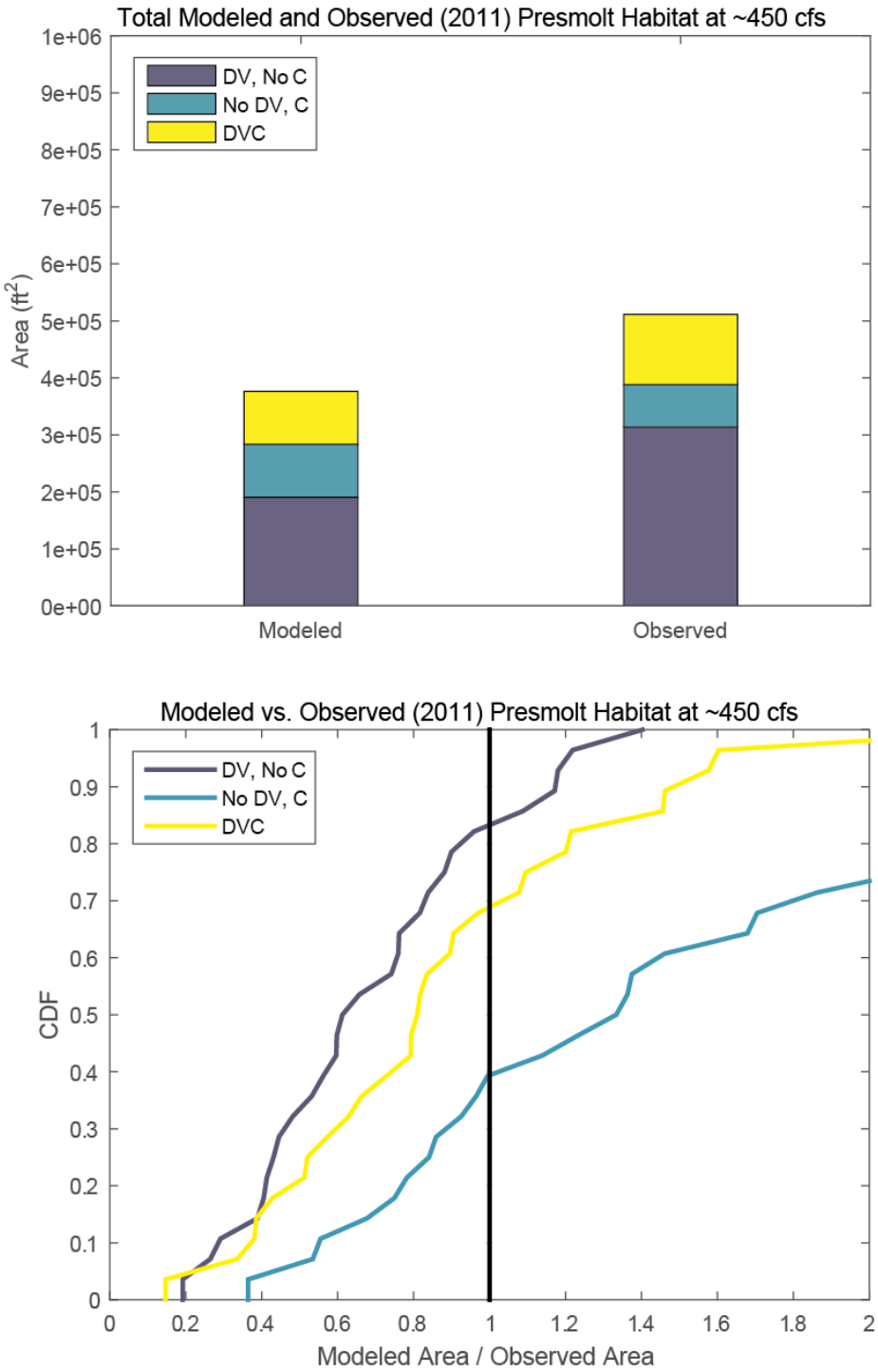

Figure 27. The 450 cfs model compared to 2011 habitat observations. The modeled DV, No C category has about 60% as much habitat area as observed and the No DV, C category has about 1.5x as much area as observed. The total amount of cover in the model (No DV, C + DVC) is similar to the amount observed in 2011, 2012, and 2013.

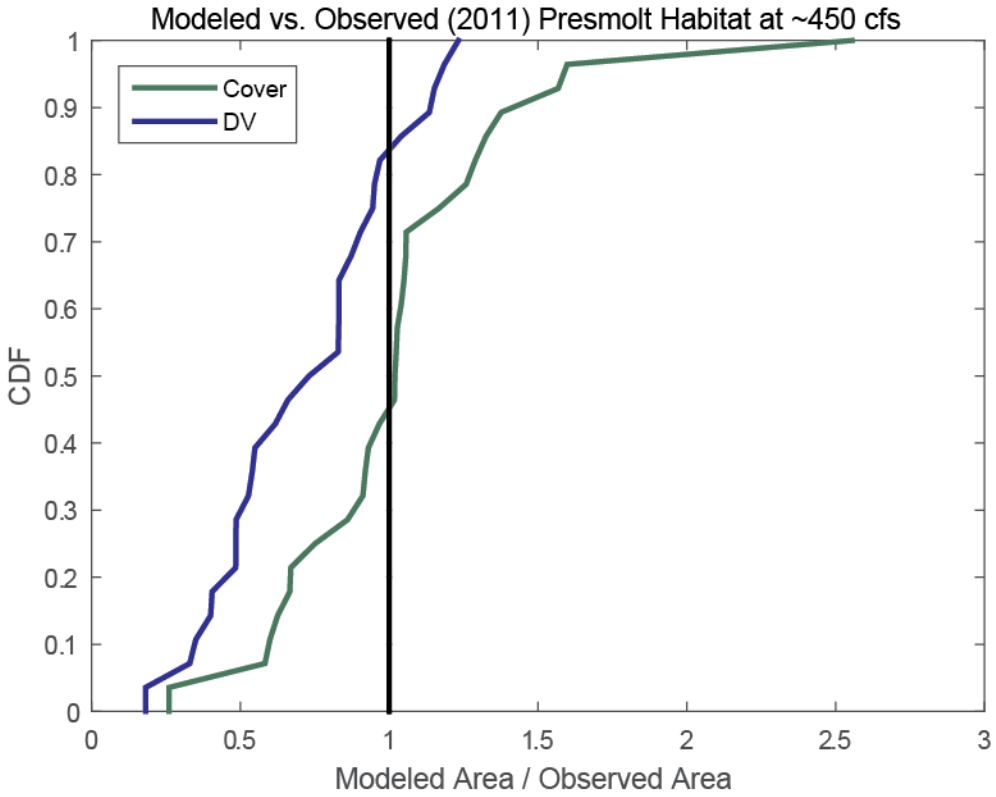

Figure 28. The distribution of the ratio of modeled to observed 2011 450 cfs habitat in the optimal depth and velocity categories (DV, No C + DVC) and the cover categories (No DV, C + DVC). The model under-estimates DV habitat in ~85% of the panels and overestimates the amount of cover in ~50% of the panels. The median ratio of DV habitat is about 0.6, similar to other years. The ratio of modeled cover to observed cover has a mode near 1, indicating that over more than 30% of the panels, the amount of cover in the model is very similar to what is observed.

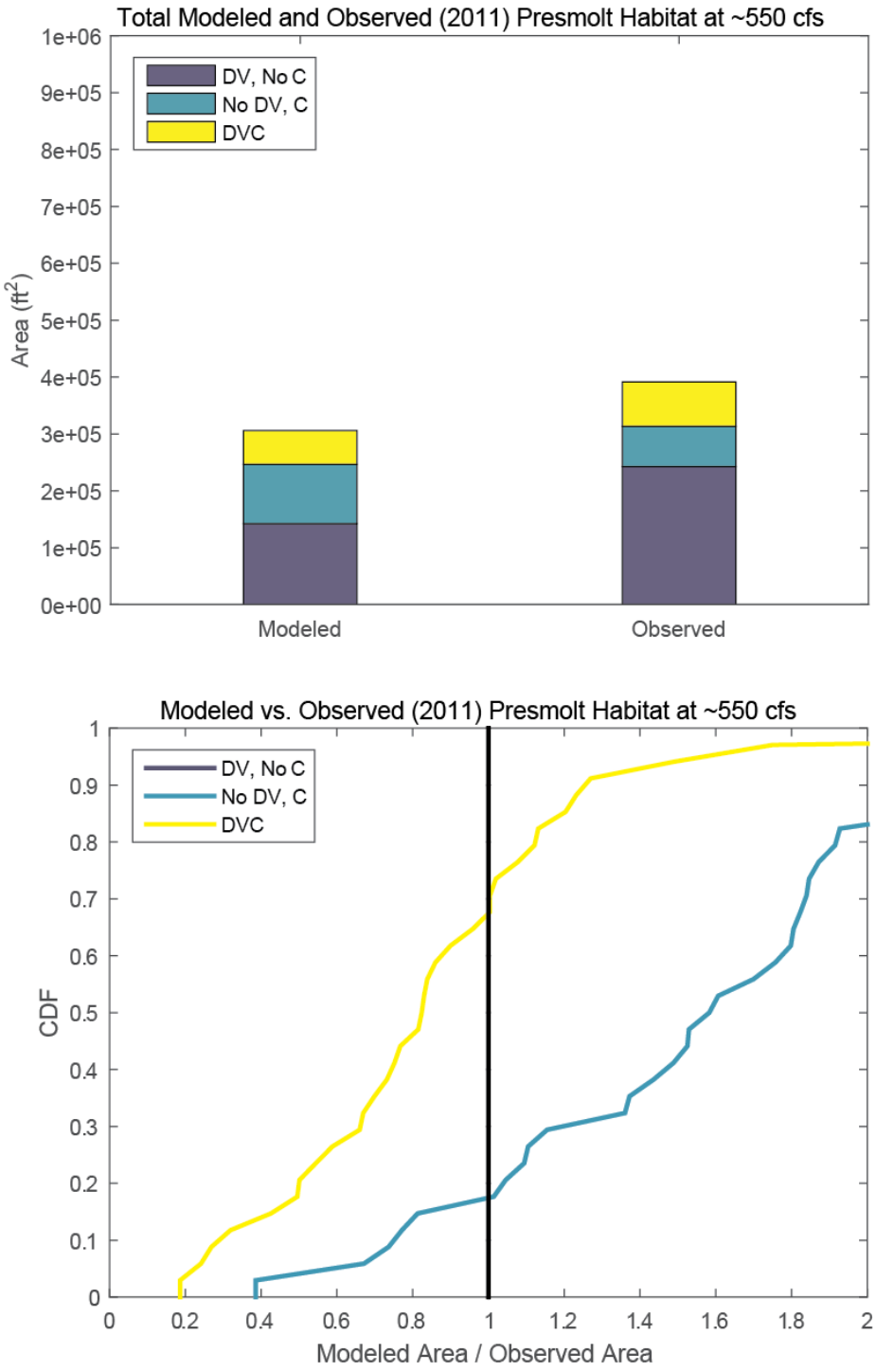

Figure 29. The 550 cfs model compared to 2011 ~550 cfs habitat observations. The modeled DV, No C category has about 60% as much habitat area as observed and the No DV, C category has about 1.5x as much area as observed.

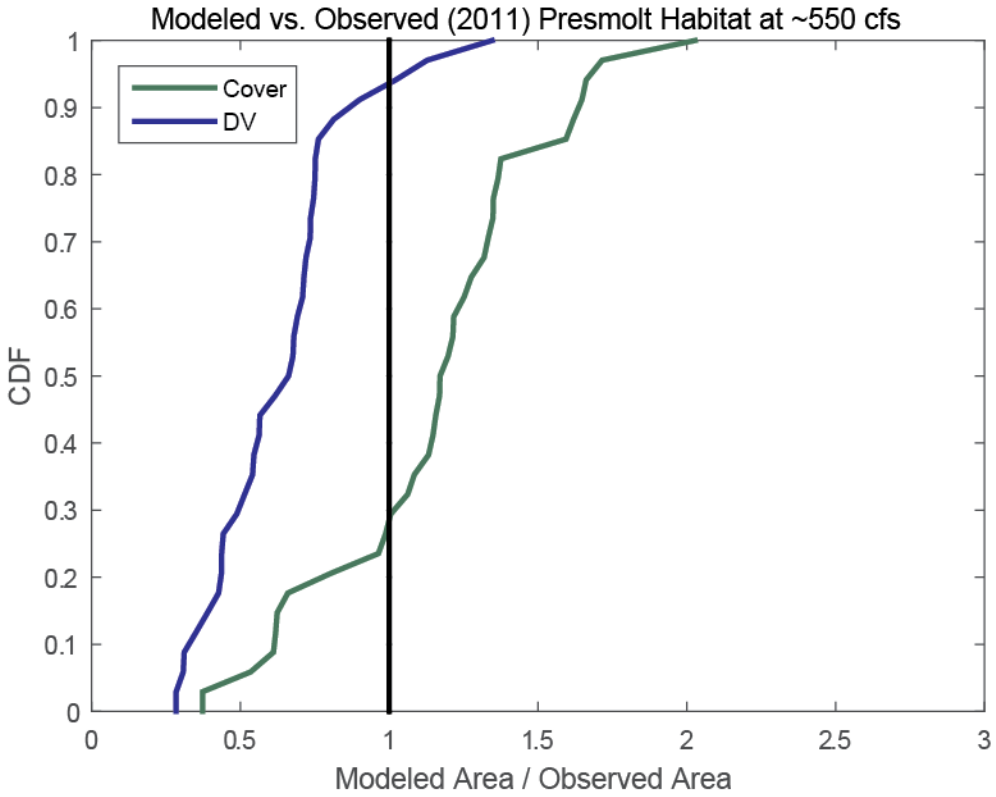

Figure 30. The distribution of the ratio of modeled to observed 2011 550 cfs habitat in the optimal depth and velocity categories (DV, No C + DVC) and the cover categories (No DV, C + DVC). The model under-estimates DV habitat in ~95% of the panels and overestimates the amount of cover in ~70% of the panels. The median ratio of DV habitat is about 0.6, similar to other years. The ratio of modeled cover to observed cover has a mode between 1 and 1.5, indicating that over about 60% of the panels, the amount of cover in the model is between 1 and 1.5x what is observed.

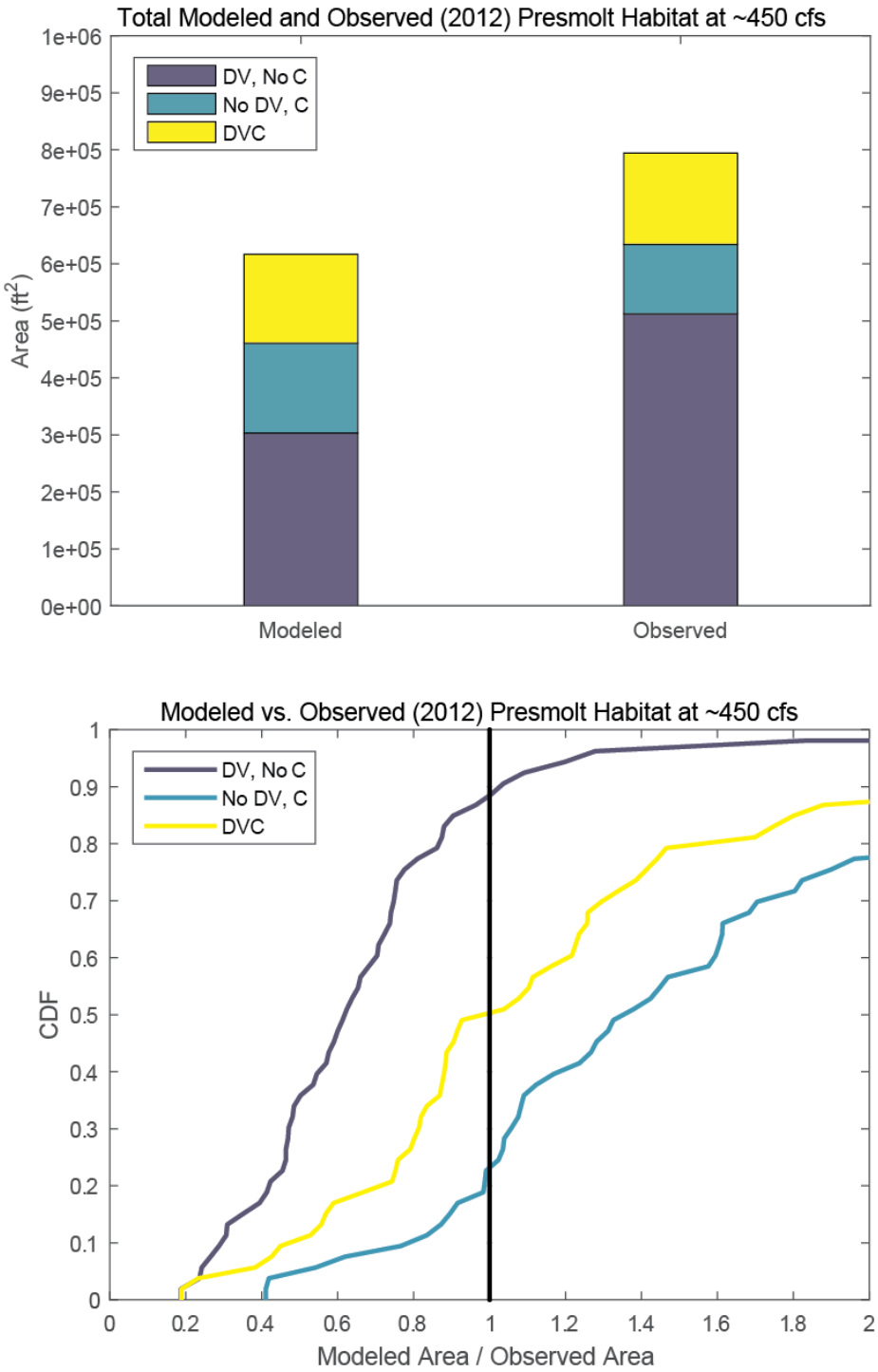

Figure 31. The 450 cfs model compared to 2012 habitat observations. The modeled DV, No C category has about 60% as much habitat area as observed and the No DV, C category has about 1.5x as much area as observed. The total amount of cover in the model (No DV, C + DVC) is similar to the amount observed.

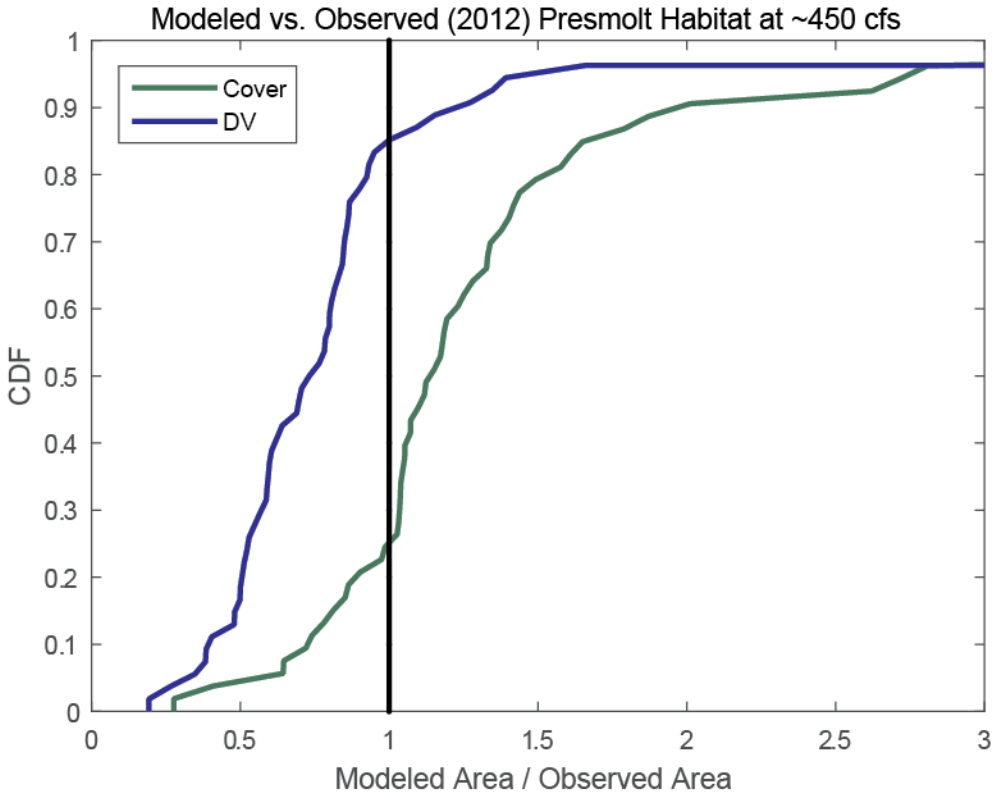

Figure 32. The distribution of the ratio of modeled to observed 2012 450 cfs habitat in the optimal depth and velocity categories (DV, No C + DVC) and the cover categories (No DV, C + DVC). The model under-estimates DV habitat in ~85% of the panels and overestimates the amount of cover in ~75% of the panels. The median ratio of DV habitat is about 0.6, similar to other years. The ratio of modeled cover to observed cover has a mode between 1 and 1.5, indicating that over about 50% of the panels, the amount of cover in the model is between 1 and 1.5x what is observed.

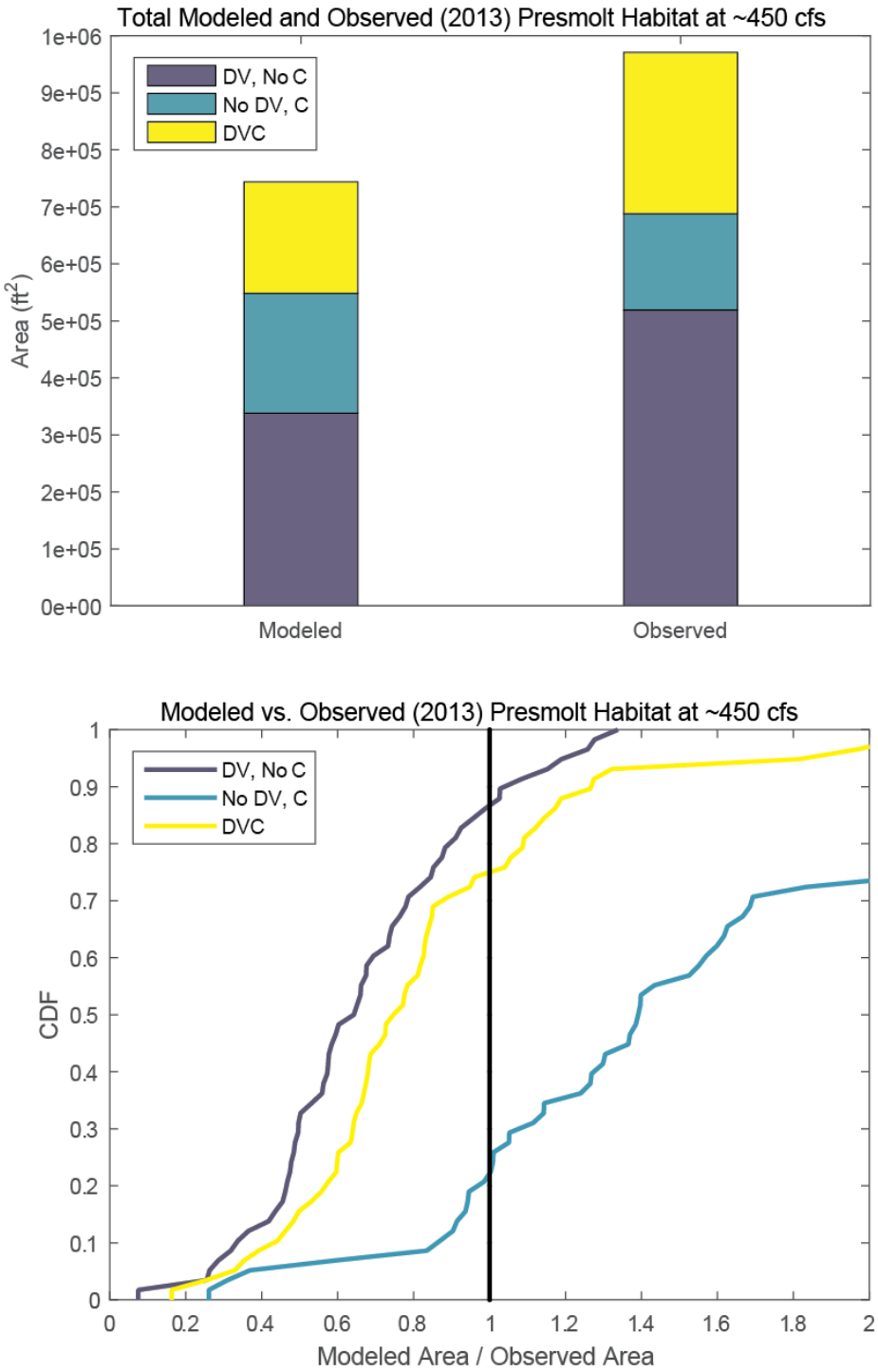

Figure 33. The 450 cfs model compared to 2013 habitat observations. The modeled DV, No C category has about 60% as much habitat area as observed and the No DV, C category has about 1.5x as much area as observed. The total amount of cover in the model (No DV, C + DVC) is similar to the amount observed.

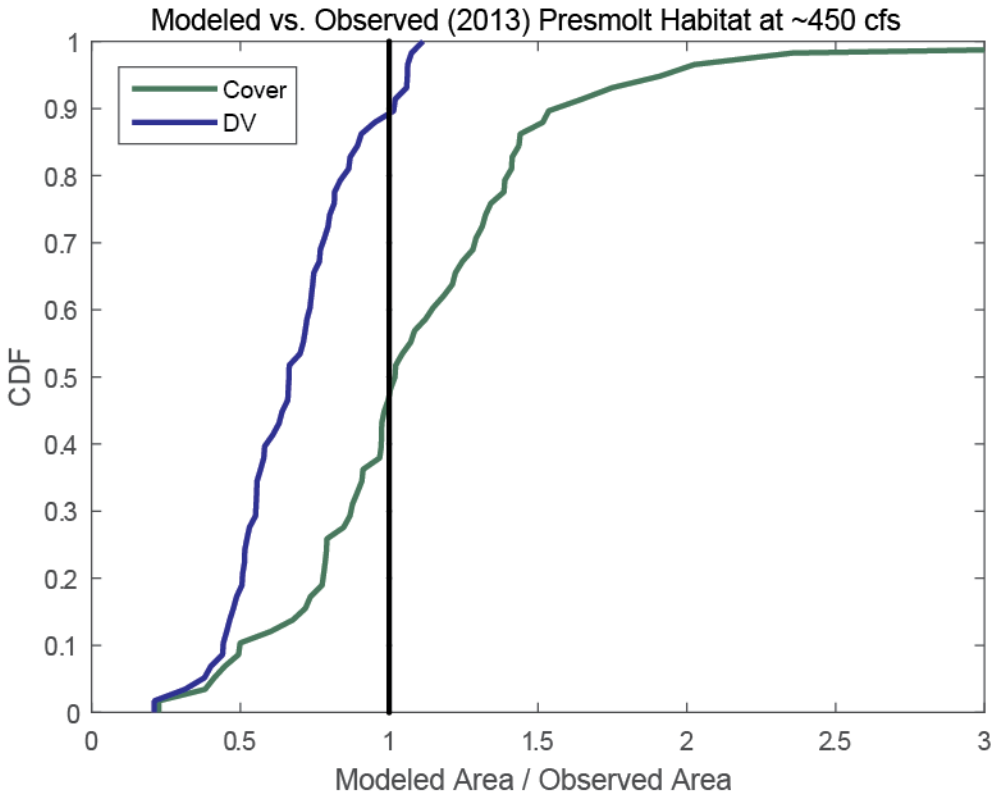

Figure 34. The distribution of the ratio of modeled to observed 2013 450 cfs habitat in the optimal depth and velocity categories (DV, No C + DVC) and the cover categories (No DV, C + DVC). The model under-estimates DV habitat in ~90% of the panels and overestimates the amount of cover in ~50% of the panels. The median ratio of DV habitat is about 0.6, similar to other years. Approximately 60% of the panels have a ratio of modeled to observed cover that is in the range of 75-125% of the amount observed.

Comparison of Categorical Habitat Using Fuzzy Kappa

The fuzzy kappa statistic is a tool for comparing two categorical raster maps. The fuzzy kappa score increases with increasing similarity between the two maps, with 1 representing perfect agreement. The similarity of the maps is scored with a matrix that gives partial credit for overlapping categories and weights the score based on the distance between similar raster cells.

For example, a raster cell representing DV, No C in one map receives a score of 0.5 when compared to a raster cell representing DVC in the second map. That score weighted by a decreasing exponential function of distance between the raster cells $f(d) = e^{-d/d_0}$, where d is the distance between the raster cells and $d_0 = 25$ ft. *Hagen* [2000] describes the scoring algorithm in detail. We modified the algorithm to allow comparison of two maps that have variable cell sizes. The sizes of corresponding cells in the two maps must be the same, but the area of cells can vary within the maps and the algorithm corrects the computation so areas of agreement or disagreement are rewarded or penalized in proportion to the ratio of cell area to total area. Because large areas of dry floodplain in both the model and observations would bias the fuzzy kappa statistic towards good agreement, we omitted cells that were dry in both the model and the observations from the calculation.

Table 5 provides qualitative guidance for interpreting the fuzzy kappa statistic. Table 5 shows the fuzzy kappa statistic of the model compared to the 450 cfs observations listed in Table 3. The 550 cfs observations were not used because those observations do not include an open water polygon in the shapefile, which is required by the computation algorithm. The average over all GRTS panels is above 0.7 for all years of habitat observations. This at the upper end of the "substantial agreement" category of *Landis and Koch* [1977]. The distributions of fuzzy kappa scores are show in Figure 35. The modal values are even higher than the averages.

Table 5. Interpreting the fuzzy kappa statistic

κ statistic	**Strength of Agreement**
<0.00	Poor
0.00 – 0.20	Slight
0.21 – 0.40	Fair
0.41 – 0.60	Moderate
0.61 – 0.80	Substantial
0.81 – 0.99	Almost Perfect
1	Perfect

Source: *Landis and Koch* [1977]

Table 6. Fuzzy Kappa statistics by panel of model compared to observations

GRTS Panel ID	2009 450 cfs	2010 450 cfs	2011 450 cfs	2012 450 cfs	2013 450 cfs
40 Mile Average	0.7521	0.7214	0.7175	0.7055	0.7650
5			0.3824	0.3605	
6			0.4636	0.5177	
13		0.8113			
14		0.7726			
15				0.6900	0.7253
16				0.7466	0.7083
17		0.7493	0.7505	0.0687	
18		0.8176	0.8690		
21			0.7334	0.7313	
22			0.5975	0.5613	
24				0.0259	
25				0.4842	0.4480
26				0.8412	0.7816
27		0.6749	0.7419		
28		0.6687	0.6680		
29		0.6670	0.7025		
30		0.6012	0.6754		
33					0.6675
34					0.5273
34					0.5717
35			0.6198	0.7026	
36			0.8174	0.8124	
41	0.7879				0.7378
42	0.6447				0.6380
47	0.7991	0.8091			
48	0.5467	0.5768			
53				0.7690	0.7806
54				0.7988	0.8474
57	0.4790	0.6911			
58	0.5813	0.7142			
59	0.7212				0.7833
60	0.6824				0.6909
63			0.7267		
64			0.7269		
67			0.7885		
68			0.7673		
71	0.7460				0.7085
72	0.8471				0.7787
75				0.8203	0.7745
76				0.7240	0.7269

79	0.7388				
80	0.7475				
83			0.8264	0.8758	
84			0.7593	0.7728	
91				0.8131	0.8060
92				0.6260	0.6192
93	0.8118				
94	0.7675				
99			0.7264		
100			0.7263		
101			0.6098	0.6621	
102			0.8268	0.8084	
103			0.6279	0.5249	
104			0.7459	0.7082	
109	0.8289				0.7200
110	0.8438				0.8416
115	0.8679				
116	0.7933				
119				0.8738	0.8261
120				0.7121	0.7483
121	0.6649				0.4773
122	0.8314				0.8338
123			0.7731		
124			0.8319		
131			0.8084	0.8697	
132			0.7966	0.8277	
133	0.8317				
134	0.6574				
134	0.7703				
135				0.8666	0.8626
136				0.8581	0.8675
141	0.8333				0.8204
142	0.7231				0.7576
143	0.7702				
144	0.7914				
147					0.8464
148					0.8637
149				0.7839	
150				0.5032	
161	0.6209				
162	0.7755				
165	0.8449				0.8164
166	0.8029				0.8450

171				0.6672	
172				0.8116	
175	0.8064				
176	0.5417				
181				0.7754	
182				0.7091	
183				0.8154	
184				0.8210	
190				0.0260	
191				0.7835	0.7966
192				0.8516	0.8007
193	0.8053				
194	0.7136				
194	0.7668				
195				0.8123	
196				0.8192	
207				0.8154	
208				0.7988	
211	0.9014				0.8271
212	0.9137				0.9073
218				0.0015	
219				0.8413	0.7809
220				0.8608	0.8028
223	0.8309	0.7927			
224	0.7885	0.7527			
225	0.8241				0.9151
226	0.8045				0.8800
231	0.7693				
232	0.8561				
235	0.8359				0.8570
236	0.8530				0.8753
243					0.8509
244					0.8631
245				0.7998	0.7842
246				0.7985	0.7762
251				0.7193	
252				0.8999	
263				0.7946	
264				0.7301	
264				0.7608	
265	0.6716				0.5424
266	0.6256				0.7308
267				0.9157	

268				0.8450	
275	0.7535				
276	0.7464				
279					0.7493
280					0.6702
289	0.5009				
290	0.7768				
295	0.7867				0.8510
296	0.7451				0.8556
297	0.6891				
298	0.7187				
301					0.7705
302					0.5627
303	0.6547				0.6907
304	0.7914				0.8329
315					0.8644
316					0.8503

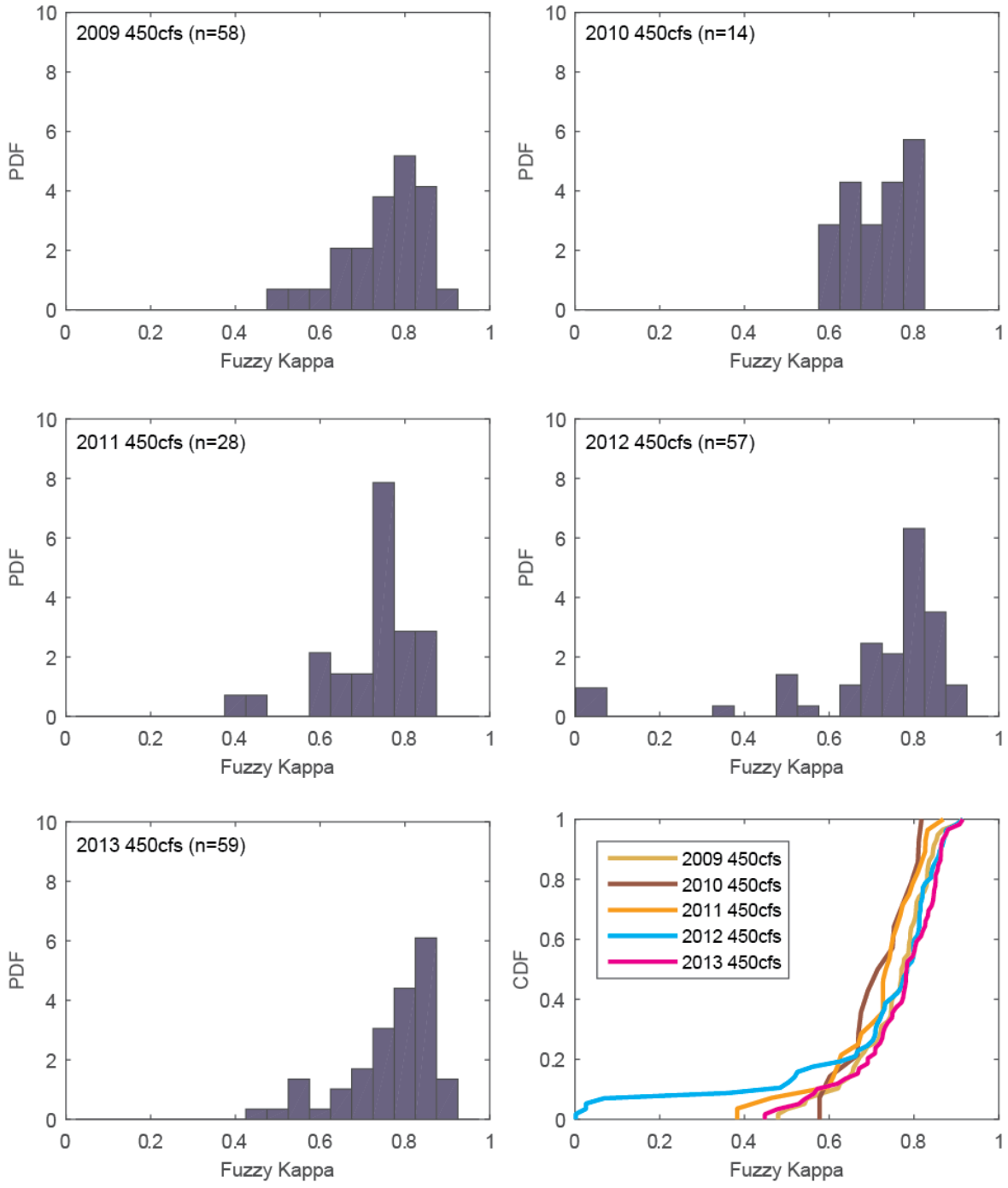

Figure 35. The distributions of fuzzy kappa scores. The bin size of the histograms is 0.05. The plot in the lower right shows the cumulative distributions. The density functions are left skewed, resulting in modes that are higher than the averages.

Summary and Conclusions

The Bureau of Reclamation's Sedimentation and River Hydraulics group has developed two versions of an SRH-2D hydraulic model of the Trinity River between Lewiston Dam and the North Fork for the TRRP since the fall of 2013. The first version of the model was calibrated to within +/- 0. 5 feet of observations of water surface elevation at a range of flows and was used in conjunction with the Hydrodynamic Based Logic Modelling Tool [*Bandrowski et al.*] to evaluate potential habitat restoration sites. Analysis of this version of the model showed that the model water velocities were significantly faster than point measurements of water velocity in the actual river and therefore the model underestimated the amount of juvenile salmonid habitat.

In an attempt to improve estimates of velocity and habitat, a second version of the model was developed which used much smaller mesh elements along the channel margins. The smaller elements reduced the area over which the model averaged depth and velocity better represented slow, shallow water along the banks. The roughness in this version of the model was derived from observations of the sediment size along the entire 40 miles (as opposed to being calibrated by guessing at values of Manning's n). It is this version of the model that is analyzed in the bulk of this report. This version of the model has been used to evaluate existing conditions in the Chapman Ranch to Sheridan Creek reach, to compare proposed restoration designs for this reach to the current conditions, and as the hydraulic input to a fish production model.

The current model is an improvement over the first version of the model. Velocity estimates are much closer to observed velocities (though still too fast) and the representation of habitat is encouraging. The differences from observed habitat are fairly systematic and stem mainly from the model's over-estimation of flow velocity. An evaluation of categorical habitat maps based on the fuzzy kappa statistic shows substantial agreement between observed and modeled habitat.

The model could be improved with by improving the bathymetric terrain model on which it is based. The resolution of the existing terrain model along the banks is lower in places than is in the center of the channel. This is due to over-hanging vegetation and under-cut banks that limited access during the bathymetric survey. This limitation may be one of the reasons that the model under-represents the amount of very slow water. In addition, the current terrain model does not include construction and natural channel changes since 2012. Bed roughness estimates based on the substrate map could be improved by incorporating water surface elevation observations along the entire 40 miles at several different flows. Confidence in the model could be improved with velocity measurements that average over a water volume similar in size to a model cell. Many of these data are being collected during the 2016 high flow and should be incorporated into a new, re-calibrated version of the model when they are available.

References

Alvarez, J., D. Goodman, K. DeJuilio, and A. Martin (2015), Substrate Map, Trinity River Restoration Program Data Package. Hoopa Tribal Fisheries, U.S. Fish and Wildlife Service, and Yurok Tribal Fisheries, Arcata, CA, http://odp.trrp.net/Data/Packages/PackageDetails.aspx?package=69.

Bandrowski, D., Y. Lai, D. N. Bradley, J. Murauskas, and D. Gaeuman (2014), 2D Hydrodynamic Based Logic Modelling Tool for River Restoration Decision Analysis: A Quantitative Approach to Project Prioritization, paper presented at AGU Fall Meeting Abstracts.

García, M. (2008), Sediment Transport and Morphodynamics, in *Sedimentation Engineering*, edited, pp. 21-163, doi:doi:10.1061/9780784408148.ch02.

Graham Matthews and Associates (2012), 2010-2012 Trinity River bathymetric mapping. Report to the U.S. Bureau of Reclamation, Trinity River Restoration Program by Graham Matthews & Associates, Weaverville, CA.*Rep.*

Hagen-Zanker, A. (2009), An improved Fuzzy Kappa statistic that accounts for spatial autocorrelation, *International Journal of Geographical Information Science*, *23*(1), 61-73, doi:10.1080/13658810802570317.

HVT, and McBain Associates (2015), Trinity River project area riparian mapping [2014 vegetation map data package], Hoopa Valley Tribe and McBain Associates, Hoopa, CA, http://odp.trrp.net/Data/Packages/PackageDetails.aspx?package=74.

Lai, Y. (2008), SRH-2D version 2: Theory and User's Manual, *Sedimentation and River Hydraulics–Two-Dimensional River Flow Modeling, US Department of Interior, Bureau of Reclamation, November*.

Landis, J. R., and G. G. Koch (1977), The Measurement of Observer Agreement for Categorical Data, *Biometrics*, *33*(1), 159-174, doi:10.2307/2529310.

López, R., and J. Barragán (2008), Equivalent Roughness of Gravel-Bed Rivers, *Journal of Hydraulic Engineering*, *134*(6), 847-851, doi:doi:10.1061/(ASCE)0733-9429(2008)134:6(847).

Som, N. A., D. H. Goodman, R. W. Perry, and T. B. Hardy (2015), Habitat Suitability Criteria via Parametric Distributions: Estimation, Model Selection and Uncertainty, *River Research and Applications*.

Woolpert, I. (2013), Trinity River bathymetry, airborne laser data and photogrammetric DTM merging, verification and certification. Report to the US Bureau of Reclamation, Trinity River Restoration Program, by Woolpert Inc., Englewood, CO.*Rep.*

Appendix A. Low Flow Tributary Accretion Data for Habitat Runs

On Tuesday, May 20th, 2014 it was decided in a meeting that tributary accretion to the Trinity River was important enough during low flow periods that it should be modeled and the effects on salmonid habitat analyzed. We decided to model the 300 cfs (at Lewiston) winter base flow period of January 1st to April 30th and the summer base flow of 450 cfs (at Lewiston) period of July 1st to Sept. 30th.

Because of variability in tributary discharge from year to year, we decided to model the 20th, 50th, and 80th percentiles of tributary discharge to represent dry, normal, and wet years. On 6/2/14, Aaron Martin and I agreedto add more percentiles to the winter baseflow model (300 cfs at Lewiston) because the results for the 20th, 50th, and 80th percentiles appeared to be wetter than the ROD defined water year types (i.e. 50th percentile looks like a wet year rather than a normal year). The new percentiles are listed in the tables below. This approach is perhaps less than representative because extensive gaging on the mainstem of the Trinity and its tributaries began only after the year 2000.

There are six major tributaries included in the model, three of which are gaged and three of which are not. The discharge on un-gaged tributaries was estimated from mainstem gage records and tributary gage records. Tributary discharge equals downstream gage minus upstream gage minus any intervening tributaries. The USGS gage data used was mean daily discharge. These 6 major tributaries are stand-ins for a number of smaller tributaries along the river (meaning that the flows from the smaller tributaries are assumed to occur at the larger ones).

Table 7. Estimating discharge for un-gaged tributaries

Tributary	**Method**
Weaver Creek	Douglas City – (Limekiln + Indian Creek)
Browns Creek	Junction City – Douglas City
Canyon Creek	Above North Fork gage near Helena

Tributary Accretion Estimates for 300 cfs (at Lewiston) period, Jan. 1 to April 30

Table 8. Gaged Tributaries and their flow at various non-exceedance percentiles for a Trinity River flow of 300 cfs.

Tributary	USGS Site No.	Period	12.5th	25th	37.5	50th (cfs)	62.5	75	87th (cfs)
Rush Creek	11525530	10/1/2002 – 5/20/2014	24	33	43	54	68	86	120
Grass Valley Creek	11525630	10/1/2004 – 5/20/2014	18	30	37	47	67	88	127
Indian Creek	11525670	10/1/2004 – 5/20/2014	12	20	28	38	54	77	117

Table 9. Gages used in estimating un-gaged tributary discharge

Gage	USGS Site No.	Period
Limekiln	11525655	4/28/1981 – 4/20/2014*
Indian Creek	11525670	10/1/2004 – 5/20/2014
Douglas City	11525854	10/1/2002 – 5/20/2014
Junction City	11526250	10/1/2002 – 5/20/2014
Above North Fork near Helena	11526400	3/29/2005 – 5/20-/2014

*****The Limekiln gage record has a gap from Oct. 1st, 1991 to Sept. 30, 2002.

Table 10. Estimated un-gaged tributary discharge at various non-exceedance percentiles for a Trinity River flow of 300 cfs.

Tributary	12.5th	25th	37.5	50th (cfs)	62.5	75	87.5
Weaver Creek	43	67	101	139	170	211	312
Browns Creek	60	100	139	202	270	362	610
Canyon Creek	89	134	163	194	250	320	472

Table 11. Tributary accretion values for 300 cfs period at various non-exceedance percentiles for a Trinity River flow of 300 cfs.

Tributary	**12.5th**	**25th**	**37.5**	**50th (cfs)**	**62.5**	**75**	**87th (cfs)**
Rush Creek	24	33	43	54	68	86	120
Grass Valley Creek	18	30	37	47	67	88	127
Indian Creek	12	20	28	38	54	77	117
Weaver Creek	43	67	101	139	170	211	312
Browns Creek	60	100	139	202	270	362	610
Canyon Creek	89	134	163	194	250	320	472
Total Accretion	**246**	**384**	**511**	**674**	**879**	**1144**	**1758**
Percent Increase due to Tribs	**82**	**128**	**170**	**225**	**293**	**381**	**586**

Tributary Accretion estimates for 450 cfs (at Lewiston) period, July 1 to Sept. 30

Table 12. Gaged tributaries and flow at various non-exceedance percentiles for a Trinity River flow of 450 cfs.

Tributary	**USGS Site No.**	**Period**	**20th (cfs)**	**50th (cfs)**	**80th (cfs)**
Rush Creek	11525530	10/1/2002 – 5/20/2014	2	3	6
Grass Valley Creek	11525630	10/1/2004 – 5/20/2014	8	11	17
Indian Creek	11525670	10/1/2004 – 5/20/2014	2	6	10

Table 13. Gages used in estimating un-gaged tributary discharge

Gage	USGS Site No.	Period of Operation
Limekiln	11525655	4-28-1981 – 4/20/2014*
Indian Creek	11525670	10/1/2004 – 5-20-2014
Douglas City	11525854	10/1/2002 – 5/20/2014
Junction City	11526250	10/1/2002 – 5/20/2014
Above North Fork near Helena	11526400	3/29/2005 – 5-20-2014

*****The Limekiln gage record has a gap from Oct. 1st, 1991 to Sept. 30, 2002.

Table 14. Estimated un-gaged tributary discharge for a Trinity River flow of 450 cfs.

Tributary	20th Percentile (cfs)	50th (cfs)	80th (cfs)
Weaver Creek*	1	18	45
Browns Creek	0	10	31
Canyon Creek	0	24	100

* Includes contributing discharge from nearby Reading Creek.

Table 15. Tributary accretion values for 450 cfs period for a Trinity River flow of 450 cfs.

Tributary	20th (cfs)	50th (cfs)	80th (cfs)
Rush Creek	2	3	6
Grass Valley Creek	8	11	17
Indian Creek	2	6	10
Weaver Creek*	1	18	45
Browns Creek	0	10	31
Canyon Creek	0	24	100
Total Accretion	13 (+3%)	72 (+16%)	209 (+46%)

* Includes contributing discharge from nearby Reading Creek.